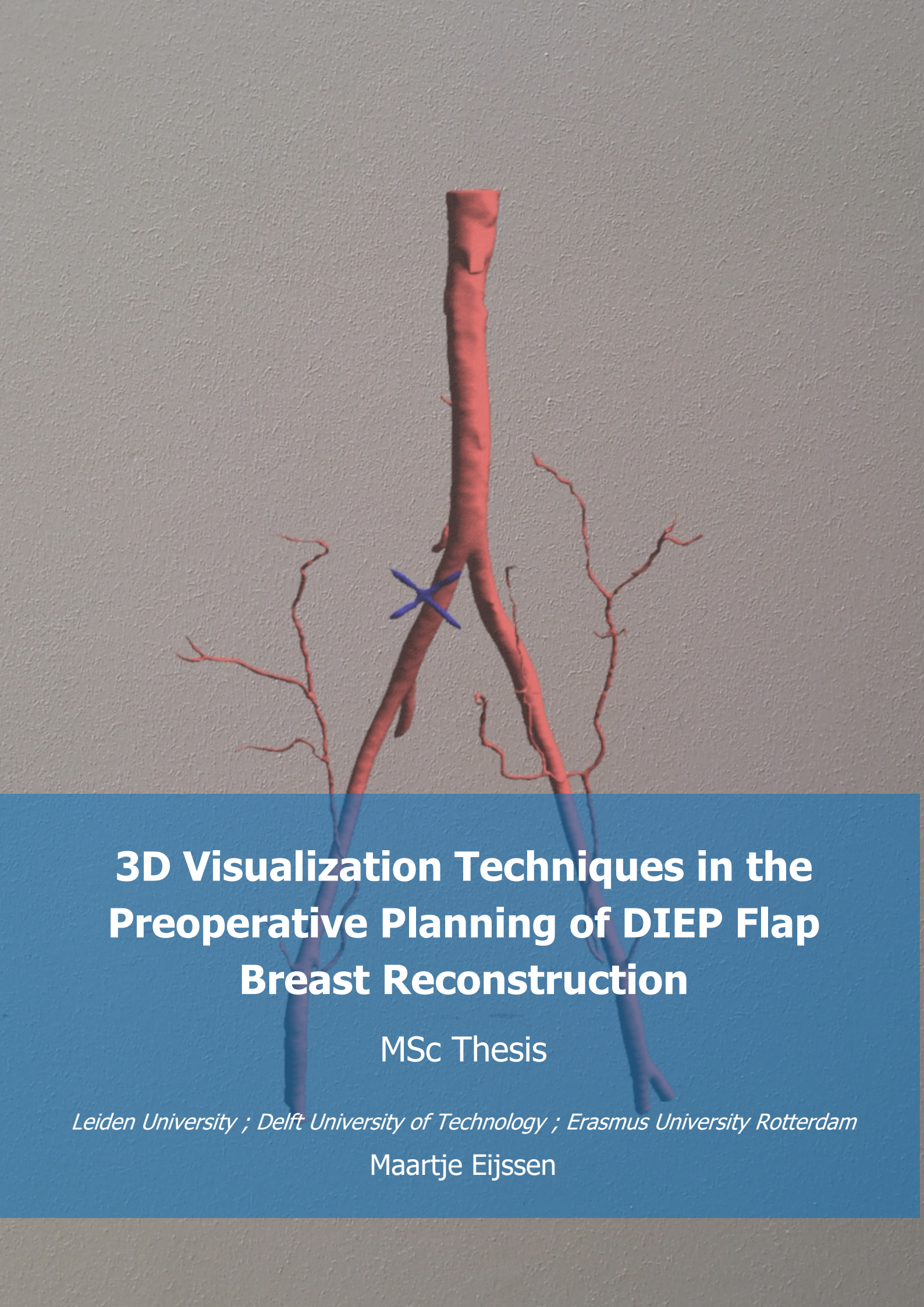

3D Visualization Techniques in the Preoperative Planning of DIEP Flap Breast Reconstruction

MSc Thesis

Leiden University ; Delft University of Technology ; Erasmus University Rotterdam

Maartje Eijssen

3D Visualization Techniques in the Preoperative Planning of DIEP Flap Breast Reconstruction

- MSc thesis -

Maartje Eijssen

18th of September 2024

Thesis in partial fulfilment of the requirements for the joint degree of Master of Science in

Technical Medicine

Leiden University ; Delft University of Technology ; Erasmus University Rotterdam

Master thesis project (TM30004 ; 35 ECTS)

Dept. of Biomechanical Engineering, TUDELFT
Dept. of Plastic Surgery, LUMC

December 2023 – September 2024

Supervisor(s):

Dr. R.P.J. van den Ende	Technical physician
Dr. R.R. Dijkman	Plastic surgeon
Drs. P.S. Verduijn	Plastic surgeon

Thesis committee members:

Dr. R.R. Dijkman, LUMC	Chair & Medical member
Dr. R.P.J van den Ende, LUMC	Technical member
Dr. B. Cornelissen, EMC	External member
Drs. P.S. Verduijn, LUMC	Medical member

An electronic version of this thesis is available at http://repository.tudelft.nl/.

Universiteit Leiden

TU Delft Delft University of Technology

Erasmus University Rotterdam

Preface and Acknowledgements

With this MSc thesis, my seven-year journey at the Technical University of Delft comes to an end. The combination of the medical and technical fields through the Bachelor's in Clinical Technology and the Master's in Technical Medicine was the perfect choice for me. I particularly enjoyed the internships during the second year of my Master's and the thesis work, which exposed me to many fascinating aspects of this field. My first internship was at the Plastic Surgery Department of LUMC, and thanks to Roy and Pieter, I knew I wanted to return to this department for my thesis. Coupled with my interest in Augmented Reality, which was sparked during my internship at the Trauma Surgery Department at EMC, this thesis was the ideal conclusion to my Master's.

I would like to thank my supervisors Roy, Robert, and Pieter for their enthusiasm and support over the past few months. The biweekly Monday meetings with Roy were always a great way to kick off the week. He asked the right questions at the right time, encouraging my critical thinking. Robert and Pieter enthusiastically introduced me to the world of plastic surgery at LUMC, and I had multiple opportunities to experience firsthand what an exceptional field this is. I also want to thank the rest of the plastic surgery team for all the experiences, clinical lessons, and help with collecting my data. Lastly, I would like to thank all my friends and family for listening to my stories about my research and the fascinating surgeries I attended.

Summary

Introduction

The Deep Inferior Epigastric Perforator (DIEP) flap is the preferred tissue flap for autologous breast reconstruction. Preoperative assessment of the DIEP flap's vascular anatomy and optimal perforator selection is crucial for flap viability. Current imaging techniques such as CTA and Doppler US are limited by their 2D representations, which can lead to uncertainty in perforator selection. Incorporating 3D visualization offers the potential to improve preoperative planning by enhancing spatial understanding and surgical decision-making.

Aim

This thesis comprises two sub-experiments. The first aimed to evaluate the clinical impact of preoperative 3D visualization of DIEP flap perforator anatomy compared to traditional CTA scans on a 2D screen. The second aimed to validate the 3D holograms using the HoloLens 2 by comparing them with intraoperative anatomy and assessing surgeons' user experience.

Methods

Study 1: Participants assessed the perforator anatomy using three viewing environments: a CTA scan on a 2D screen, a 3D model on a 2D screen, and a 3D hologram with Augmented Reality (AR). They identified the optimal perforator and completed a questionnaire on perforator visibility, characteristics selection criteria, intraoperative confidence, and clinical applicability.
Study 2: Participants performed surgery according to clinical standards. Postoperatively, they used the HoloLens to visualize the 3D holograms. Perforator locations were documented, and the margin of error was calculated. A questionnaire evaluated the correspondence between the 3D hologram and intraoperative findings and assessed the usability of the HoloLens.

Results

Study 1: 15 patients and 3 surgeons were included. Optimal perforator selection agreement increased from 53% with CTA scans to 87% with 3D models and remained stable for AR. Correspondence with intraoperative findings improved from 75% to 92% using 3D models. Visibility scores significantly improved ($p<0.001$) for 3D visualization, and AR was the most preferred technique for clinical use.
Study 2: Three patients and 3 surgeons were included. Concordance in perforator selection improved from 1 out of 3 with CTA scans to 3 out of 3 with AR. The 3D hologram correspondence scores were >4 for all characteristics. The HoloLens received a mean SUS-score of 83.3. The margin of error was 0.8 cm for radiology reports, 0.2 cm for the 3D model, and 2.8 cm for preoperative marking.

Conclusion

3D visualization of the DIEP flap perforator anatomy enhanced the visibility of perforator characteristics, improved consensus among surgeons, and increased confidence in perforator choice. AR offers superior visualization and is preferred for clinical practice. The 3D hologram demonstrated high correspondence with intraoperative findings and improved perforator selection agreement. The usability of the HoloLens was rated as excellent, and participants expressed a strong preference for using AR in preoperative planning.

Content

1. General Introduction 7
   1.1 Clinical Background 7
   1.2 Current Process and Limitations 7
   1.3 Goals and Objectives 8
   1.4 Thesis outline 8
2. Clinical and Technical Background 10
   2.1 Clinical Background 10
      2.1.1 DIEP Flap Anatomy 10
      2.1.2 DIEP Flap Procedure 11
   2.2 Technical Background 12
      2.2.1 Augmented Reality and Mixed Reality 12
      2.2.2 The HoloLens2 13
      2.2.3 MIP Reconstructions 14
3. *'The added value of 3D visualization in the preoperative planning of DIEP flap breast reconstruction'* 15
   1. Introduction 15
   2. Methods 16
      2.1 Patients 16
      2.2 Imaging Pipeline 16
      2.3 Participants 17
      2.4 Study Design 17
   3. Results 19
      3.1 Perforator Choice 19
      3.2 Questionnaire 19
   4. Discussion 23
      4.1 Interpretation of Results 23
      4.2 Strenghts and Limitations 24
      4.3 Future Perspectives 24
   5. Conclusion 24
4. '*The clinical validation and usability of Augmented Reality in DIEP flap breast reconstruction; a pilot study*' 26
   1. Introduction 26
   2. Methods 27
      2.1 Patients 27
      2.2 Imaging Pipeline 27
      2.3 Participants 27
      2.4 Study Design 28
   3. Results 30
      3.1 Perforator Choice 30
      3.2 Perforator Number 30
      3.3 Questionnaire 31
      3.4 Margin of Error 31
   4. Discussion 32
      4.1 Interpretation of Results 32
      4.2 Strenghts and Limitations 32
      4.3 Future Perspectives 33
   5. Conclusion 33
Appendix 37
   A. Literature Review 37
   B. Study 1 Quesionnaire 53
   C. Comments and Additional Remarks Study 1 56
   D. 3D models and Perforator Labels (Study 1&2) 57
   E. Study 2 Questionnaire 60
   F. Segmentation and HoloLens Guideline 62

Chapter 1: General Introduction

1.1 Clinical background

Breast cancer is the most prevalent malignant tumor among women globally [1]. This disease accounted for approximately 12% of all new cancer cases in 2020, affecting an estimated 7.8 million women worldwide [2]. Surgery is the main treatment option for breast cancer, typically involving either breast conservation surgery (BCS) or mastectomy. BCS involves removing the malignant tumor and a small margin of surrounding healthy tissue, while in mastectomy the complete breast is removed [3].

Women undergoing breast reconstruction after mastectomy show enhanced psychosocial and sexual well-being and improved quality of life, compared to those without subsequent reconstruction [4]. Reconstructive surgery options include either implant-based methodologies or autologous tissue transfer employing a free flap technique. This latter approach utilizes the patient's tissue and is associated with higher patient satisfaction compared to implant-based reconstructions [5], [6]. The most common tissue flaps for breast reconstruction are the rectus transversus abdominis musculocutaneous (TRAM) flap and the deep inferior epigastric perforator (DIEP) flap [7]. The TRAM flap involves removing all or part of the rectus abdominis muscle, while the DIEP flap uses only skin and fat tissue, preserving the muscle and its nerves [8]. The DIEP flap leads to fewer complications and a shorter hospital stay, making it the preferred choice for reconstruction [9].

In free flap surgery, the correct identification and dissection of the Deep Inferior Epigastric Artery (DIEA) and its perforator vessels is essential for flap viability and diminishing postoperative fat necrosis [10], [11]. One or more dominant perforator vessels are identified and dissected along their intramuscular course. Important characteristics in the selection of the dominant perforator are the location of the perforator in the flap, calibre, intramuscular course through the rectus abdominis muscle, perforator origin, subcutaneous branching pattern, and the perforator's position concerning other vessels [12].

A preoperative understanding of the highly variable vascular anatomy of the DIEP flap helps in predicting the optimal perforator, reduces operative time and postoperative complications, and increases the surgeon's confidence [13]. Additionally, it reduces the risk of unforeseen selection of a different perforator or switching to an alternative flap type during surgery. During flap elevation, the first encountered perforator might appear sufficient, necessitating a choice between using it or continuing to search for the preoperatively identified optimal perforator [14].

1.2 Current process and limitations

Imaging techniques such as computed tomography angiography (CTA), magnetic resonance angiography (MRA), and Doppler ultrasonography (Doppler US) are preoperatively performed to visualize and select the optimal perforator. Although these methods effectively identify suitable perforators, they are limited by a 2D representation and require the surgeon to mentally reconstruct a 3D map of the vascular structures and their intramuscular course. Furthermore, these techniques lack direct translation from the computer screen to the corresponding anatomical location on the patient [15]. In the preoperative perforator

delineation process, the surgeon uses a handheld Doppler to mark the selected perforator(s) on the patient's abdomen. However, when using the Doppler, it is not possible to differentiate between a signal originating from the fascial penetration point and an arterial subcutaneous signal [16].

Recent advancements in alternative techniques significantly improved the perforator visualization and translation of preoperative planning into surgery. A preceding review (Appendix A) focusing on the quantitative outcomes of techniques that employ post-processing volumetric data (CTA or MRA) for perforator mapping in DIEP flap breast reconstruction surgery showed the most promising results for Augmented Reality (AR) regarding perforator identification, accuracy, and surgical efficiency.

AR could potentially improve preoperative DIEP perforator planning in two ways. First, AR shows the perforator anatomy in 3D, which has been confirmed to enhance visualization and increase the surgeon's proficiency in tracking vascular pathways, assessing their proximity to anatomical landmarks, and evaluating their course [11], [17]. The enhanced 3D visualization may influence the preoperative decision-making process, including the selection of the dominant perforator, choice of flap type, or adjustments in the intraoperative approach. Second, AR integrates virtual elements with the real-world environment, allowing for the projection of the preoperative 3D visualizations of the perforator anatomy onto the patient's body [18]. This direct overlay facilitates the translation of the preoperatively selected perforator location to the patient, potentially increasing the accuracy of preoperative perforator marking and reducing pre- and intraoperative times and complications.

1.3 Goals and Objectives

This thesis is divided into two different sub-experiments, each delineating its own goals and objectives. The goal of the first study was to evaluate the added value and clinical impact of the 3D visualization of the DIEP flap perforator anatomy compared to the traditional 2D visualization of CTA scan on a 2D screen. This study specifically compared three different viewing environments: the conventional CTA scan on a 2D screen, a 3D model on a 2D screen, and a 3D hologram using AR. The objectives of this study were to determine the impact of the viewing environment on the dominant perforator choice and the certainty of the surgeon on this choice, evaluate the surgeon's experience on the visibility of important perforator characteristics, and assess the surgeon's opinion on implementation in clinical practice.

The goal of the second study was to validate the 3D hologram using AR by comparing it with intraoperative patient anatomy. The study assessed the correspondence between the 3D hologram and the actual patient anatomy by examining the key perforator characteristics. Additionally, quantitative metrics such as the intraoperative used perforator, perforator location, and the total number of perforators were compared. Furthermore, the System Usability Score (SUS) was used to evaluate the surgeon's experience and satisfaction with using the Hololens.

1.4 Thesis outline

This chapter provided an initial outline of the clinical background, current processes and limitations, and the goals and objectives of this thesis. Chapter 2 elaborates on the clinical

background of DIEP flap anatomy and the surgical procedure, as well as the technical background of Augmented Reality and the HoloLens. Chapter 3 evaluates the added value of 3D visualization in the preoperative planning of DIEP flap breast reconstructions by comparing it with the conventional CTA scan on a 2D screen. Chapter 4 describes the validation of 3D holograms of DIEP flap perforator anatomy using the HoloLens 2 by comparing them with intraoperative patient anatomy. Additionally, it evaluates surgeons' user experience and satisfaction with the device.

Chapter 2: Clinical and technical background

2.1 Clinical background

2.1.1 DIEP flap anatomy

The primary flaps utilized for abdominal reconstruction include the rectus transversus abdominis musculocutaneous (TRAM) flap, the superficial inferior epigastric artery (SIEA) flap, and the DIEP flap [19]. While the TRAM flap involves the removal of part or all of the rectus abdominis muscle, the DIEP flap preserves the muscle and its nerves by only employing skin and fat tissue [8]. The DIEP flap demonstrates fewer complications and a shorter hospital stay, making it the preferred choice for reconstruction [9].

Blood supply to the flap originates from the deep inferior epigastric arteries (DIEA) and its perforator vessels [20]–[22]. Originating from the external iliac artery, the DIEA courses between the rectus sheath and rectus muscle [23]. There are three general branching patterns of the DIEA: Type 1, a single vessel; Type 2, a bifurcated vessel; and Type 3, a trifurcated vessel [14]. DIEA perforators most frequently manifest as Type 2, distributed in a medial and lateral row [24]. The different perforator patterns are illustrated in Figure 1. The venous perforators located within the rectus sheath terminate in the deep inferior epigastric veins (DIEVs), which subsequently drain into the external iliac vein. Through anastomoses, the DIEV perforator system connects to the superficial inferior epigastric vein (SIEV), which drains the subcutaneous anterior abdominal wall [25].

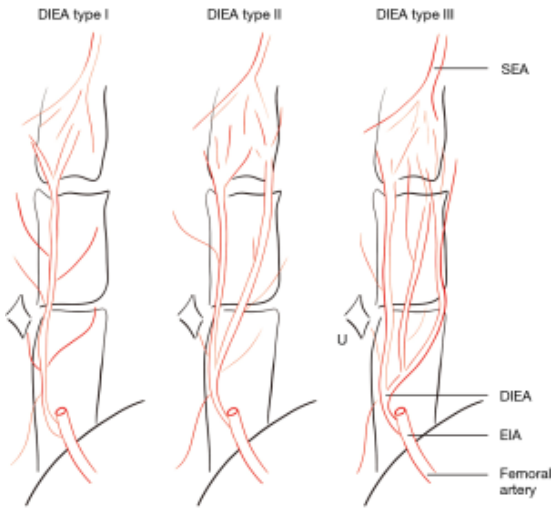

***Figure 1**: Moon and Taylor classification depicting the branching pattern of the DIEA. Type I: single vessel; type II: bifurcating vessel; type III: trifurcating vessel [Redrawn by Vivian B. Boer after Moon and Taylor].*

The perforating vessels pass the rectus muscle in a tortuous or direct course, varying in length [19]. The optimal perforator is characterized by a short intramuscular course through the rectus muscle, offering the easiest and safest dissection [23]. In cases where multiple perforators are chosen for flap perfusion, rectus abdominis fibers are spared by using perforators with a reduced intramuscular transverse course compared to each other. Once penetrating the muscle, a variety of branching patterns with an average of five (plus or minus two) perforators

supply the skin. The majority of perforating vessels are found within 2 cm cranial and 6 cm caudal and between 1 to 6 cm around the lateral aspect of the umbilicus [26].

2.1.2 DIEP flap procedure

At the Leiden University Medical Center (LUMC), preoperative visualization of the perforator vessels is achieved through computed tomography angiography (CTA) of the abdomen. Each CTA scan is reviewed by a radiologist, an Imaging Services Group (ISG) staff member, and the attending plastic surgeon. The radiology report describes the locations of the most optimal perforators for the DIEP flap relative to the umbilicus, both in the sagittal and transverse directions. Ultimately, the definitive selection of the optimal perforator is done by the plastic surgeon.

The surgeon employs a handheld Doppler in the preoperative setting to detect and demarcate the selected perforator(s) on the patient's abdomen using a surgical marker. However, Doppler signals cannot differentiate between a signal originating from the fascial penetration point or arterial subcutaneous sources [27]. Furthermore, the Doppler may detect the signal at an angle rather than perpendicular to the fascial penetration point, resulting in a discrepancy between the actual location and the marking point. Therefore, it is crucial to accurately identify the exact location of the perforator during intraoperative flap elevation. Both examples are illustrated in a figure from Berger et al. [17], depicted in Figure 2.

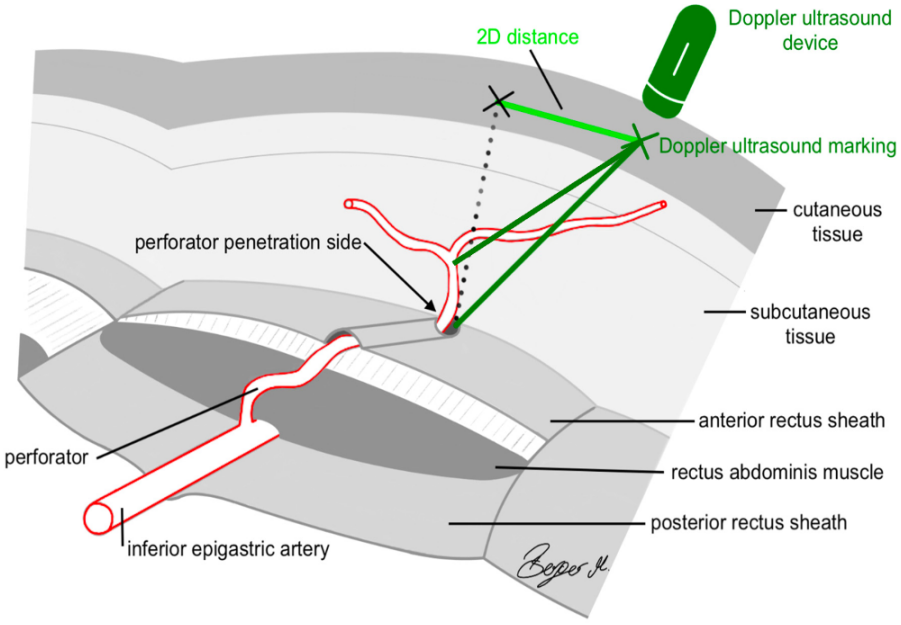

Figure 2: *The handheld Doppler can detect the perforator penetration point at an angle or identify a point in the subcutaneous fat tissue, resulting in a difference between the actual perforator location and the Doppler ultrasound marking [17].*

During surgery, the lower incision is executed to preserve the superficial inferior epigastric vein with maximal length. This allows the option for a second venous anastomosis when a flap requires additional venous drainage due to venous insufficiency [28]. The incision extends down to the abdominal fascia while preserving the Scarpa's fascia. The flap is elevated from lateral to medial in the search for the perforators [29]. As the surgeon approaches the perforator's point of penetration through the fascia, it is preferred to align the perforator with the dissection route. This ensures that the perforator becomes visible within the subcutaneous

fat during the elevation of the flap, as illustrated in Figure 3. Preoperative knowledge of the perforator anatomy allows the surgeon to adjust the surgical approach accordingly when nearing the perforator.

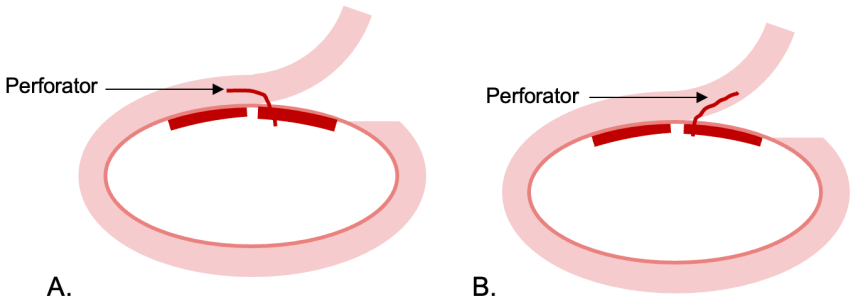

Figure 3: *Scenario A: The perforator diverges from the dissection route, making it not visible during dissection. Scenario B: The perforator aligns with the dissection route, enhancing its visibility during the procedure.*

After locating the selected perforator(s), the rectus fascia is incised around the perforator, and the intramuscular course is dissected towards the DIEA pedicle. After isolating the flap on the perforator and DIEA/DIEV and preparing the recipient site, the subcutaneous tissue and skin for reconstruction are transplanted to the recipient breast and connected with the internal mammary vessels [30]. The different steps of the DIEP procedure are schematically illustrated in Figure 4.

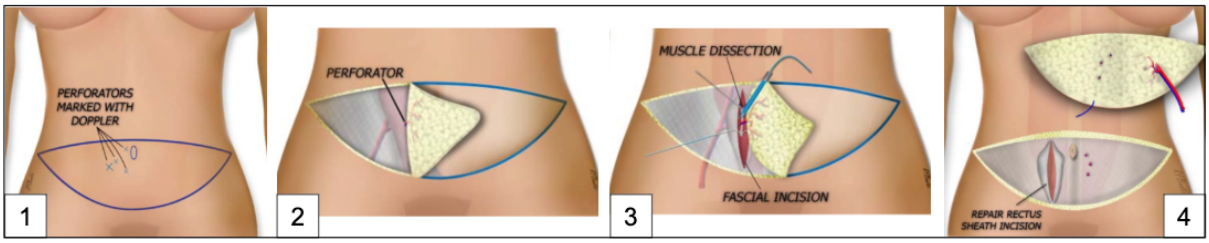

Figure 4: *The different steps in the DIEP flap procedure; (1) Marking the perforator locations on the patient's abdomen. (2) Flap elevation from lateral to medial. (3) Muscle dissection and isolating the perforator. (4) Flap transplantation to the breast [30].*

2.2 Technical background

2.2.1 Augmented Reality and Mixed Reality

Developments in medical applications of Virtual Reality (VR), Augmented Reality (AR), and Mixed Reality (MR) have aimed to improve preoperative and intraoperative visualization and guidance [31]. Virtual Reality (VR) is known to replace the real world with a digital one, immersing users in a reproduced or alternative reality. Augmented Reality (AR) projects virtual objects as holograms into the real-world environment but is limited to the visualization of 3D holograms only. Mixed Reality (MR) blends both the physical and digital worlds, allowing users to directly interact with virtual objects and information [32]. Figure 5 shows the mixed reality spectrum [33]. Despite the difference between AR and MR, the terms MR and AR are used interchangeably in many recent studies [18]. Because the term AR is most commonly used in articles, this study will also use the term AR.

AR is categorized into three different types: projection-based, video-see-through (VST), and optical-see-through (OST) [34]. In projection-based AR, a 2D or 3D image is projected onto

the site of interest. In VST, the digital content is superimposed on a live video feed of the real world. This can be displayed on a monitor, tablet, or phone screen. In OST, the digital content is projected onto an optically clear lens that the user can see through. This is typically accomplished via a head-mounted display (HMD) such as the Magic Leap (Magic Leap, Plantation, Florida, USA) or the Microsoft Hololens (Microsoft, Redmond, Washington, USA) [34]. HMDs allow surgeons to move around and access information hands-free [35].

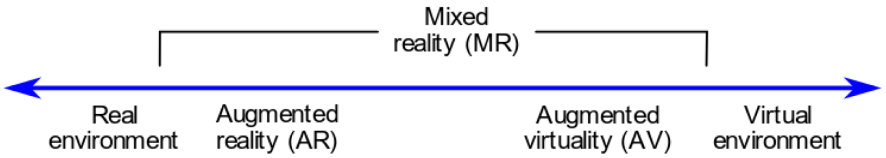

Figure 5. *The Mixed Reality spectrum, combining the physical and digital world [32].*

2.2.2 The HoloLens 2

This thesis employs the HoloLens 2 as the OST-HMD-AR device. The HoloLens has several sensors, lenses, and holographic projectors, enabling reconstruction of the real environment and creating a detailed understanding of the physical space around the user. The main components of the HoloLens 2 are listed below and are illustrated in Figure 6 [36]:

- **Four gray-scale environment tracking cameras**: Two of the gray-scale cameras are configured as a stereo rig capturing the area in front of the device so that the absolute depth of tracked visual features can be determined through triangulation. Meanwhile, the two additional gray-scale cameras provide a wider field of view to keep track of features. These cameras create a detailed understanding of the user's surroundings, facilitating accurate spatial mapping and interaction with virtual content.
- **Depth camera**: The depth camera uses active infrared (IR) illumination to determine depth through time-of-flight (ToF) technology. The camera operates in two modes, enabling near-depth sensing for hand tracking and far-depth sensing for spatial mapping [37]. Depth information is crucial for understanding the spatial layout and enabling interactions with virtual objects.
- **Inertial Measurement Unit (IMU)**: The IMU consists of sensors like accelerometers and gyroscopes that measure the device's motion and orientation in three-dimensional space. This information is used for stabilizing virtual content and ensuring accurate spatial tracking, allowing virtual objects to remain anchored in the real world as the user moves around.
- **Eye Tracking Sensors**: These sensors track the direction and movement of the user's eyes. This capability supports advanced functionalities such as foveated rendering. In foveated rendering, graphics are displayed primarily in the central area of the user's visual field, where the eye naturally focuses.
- **RGB camera**: This camera captures color images of the environment. This can be used for purposes such as image recognition, object tracking, and video recording.

The Simultaneous Localization and Mapping (SLAM) algorithms use the sensor data to help determine the HoloLens' position and orientation within the environment. This is achieved by continuously comparing the sensor data with a map of the surroundings that the device is building in real-time. By matching observed features in the environment with those in the map, the device can estimate its current location relative to the known features.

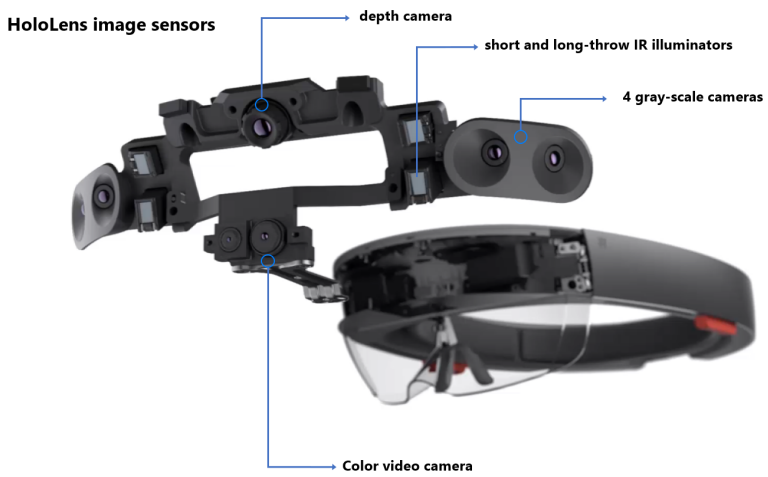

Figure 6. *The different components of the HoloLens2 [36].*

2.2.3 MIP reconstruction

For the CTA scans used in this research, the Maximum Intensity projection (MIP) reconstruction was available. MIP is a volume rendering technique that projects the highest intensity voxels along lines projected through multiple thin-slice images onto a single 2D plane, creating a slab visualizing the highest-intensity structures. MIP leverages the higher intensity values of vascular structures compared to surrounding tissue within CTA datasets. In preoperative DIEP flap planning, MIP allows for a clearer visualization of the blood vessels' course, even if they are tortuous [38-40]. An example of the MIP reconstruction for vascular structures is shown in Figure 7.

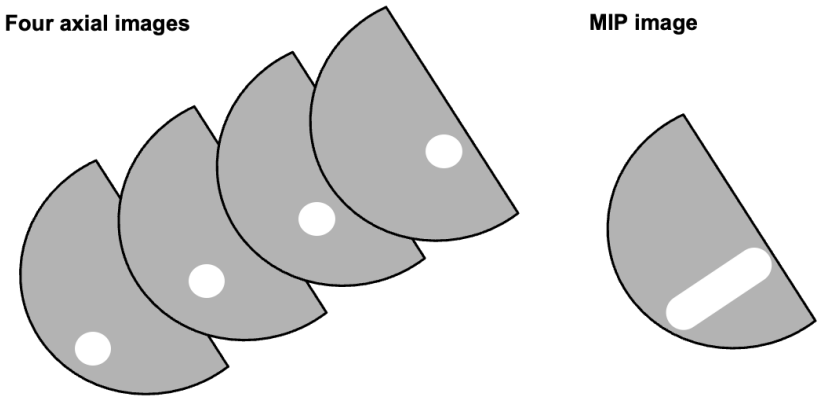

Figure 7. *An example of a MIP reconstruction for four axial images containing segments of vessels (white shapes). The MIP image (slab) combines the four axial images so that the vessel is seen in its entirety.*

Chapter 3: The added value of 3D visualization in the preoperative planning of DIEP flap breast reconstruction

1. Introduction

The Deep Inferior Epigastric Perforator (DIEP) flap is the preferred flap of choice for free flap breast reconstruction [9]. The DIEP flap utilizes the abdominal skin and fat tissue while preserving the rectus abdominis (RA) muscle and its nerves [8]. The correct identification and dissection of the Deep Inferior Epigastric Artery (DIEA) and its perforator vessels is essential for flap viability and diminishing postoperative fat necrosis [10], [11]. One or more dominant perforator vessels are identified and dissected along their intramuscular course, ensuring adequate pedicle length while preserving muscle functionality and minimizing donor site morbidity [12].

A preoperative understanding of the highly variable vascular anatomy of the DIEP flap aids in predicting the optimal perforator. Perforator characteristics considered in selecting the optimal perforator include the location of the perforator in the flap, calibre, intramuscular course through the RA muscle, perforator origin, subcutaneous branching pattern, and the position concerning other vessels [13]. Preoperative selection of the optimal perforator reduces operative time and postoperative complications while increasing the surgeon's confidence. Furthermore, it reduces the risk of inadvertent perforator selection or switching to an alternative flap type during surgery [14].

Imaging techniques such as computed tomographic angiography (CTA), magnetic resonance angiography (MRA), and Doppler ultrasonography (Doppler US) are preoperatively performed to assist in visualizing and identifying the optimal perforator. Although these methods effectively identify suitable perforators, they are limited by their 2D representation, necessitating surgeons to mentally reconstruct a 3D map of the vascular structures and their intramuscular course. This may result in uncertainty in identifying the optimal perforator and a diminished spatial understanding of the entire course of the perforator [15].

The incorporation of 3D models of the DIEP flap anatomy holds the potential to refine the preoperative understanding of perforator anatomy and thereby improve DIEP flap planning [22]. 3D visualization enhances the surgeon's proficiency in tracking vascular pathways, assessing their spatial relationships to each other and anatomical landmarks, and evaluating their course [11], [22]. This may influence the preoperative decision-making process, including the selection of the dominant perforator, choice of flap type, or adjustments in the intraoperative approach. This study aims to compare the 3D visualization of DIEP flap perforator anatomy with the conventional 2D visualization of CTA scans on a 2D screen. The assessment focuses on preoperative perforator selection, the visibility of perforator characteristics, and the confidence levels in perforator selection. Specifically, a 3D model on a 2D screen and a 3D hologram using Augmented Reality (AR) are compared with the scan on a 2D screen.

2. Method

2.1 Patients

Patients on the waiting list for single or double autologous breast reconstruction using a DIEP flap at the Leiden University Medical Center (LUMC) were included.

2.2 Imaging pipeline

2.2.1 Imaging

Routinely acquired CTA scans for the preoperative planning of DIEP flap reconstructions were utilized. The scans were acquired with either a Canon Aquilion ONE PRISM edition or a Canon Aquilion ONE GENESIS edition (slice thickness 0.5-1.0 mm, pixel spacing 0.782-1.949 mm, 100 kVp, tube current 83-425 mA, exposure time 500 ms). Maximum Intensity Projection (MIP) reconstructions with a slab thickness of 5 mm in axial, sagittal, and coronal directions were available. The scans of the included patients were anonymized before being used in the study.

2.2.2 3D model generation

Patient-specific 3D models of the perforator anatomy, RA muscle, and fat tissue were created for each patient by one researcher. To account for the learning curve, the first 5 segmentations were checked by a plastic surgeon. Raw DICOM data of the preoperative CTA scan was uploaded into the image processing software 3DSlicer (v.5.0.3, Surgical Planning Laboratory, Brigham and Women's Hospital, Boston, MA, USA) for segmentation of the structures. The vascularization, RA muscle, and fat tissue were initially segmented using 'thresholding'. The threshold value was based on the trade-off between correctly segmenting the tissue of interest and diminishing noise. The segmentations were manually corrected by the researcher. Due to low contrast within the fat tissue, the subcutaneous vascular branching pattern was not included in the initial segmentation but was manually segmented. When in doubt about the presence of a perforator, the Maximum Intensity Projection (MIP) scan was used for verification. The model was checked against the radiology report to ensure that all optimal perforators identified in the report were at least segmented. The segmentations were exported as STL files and imported into the 3D modeling software Materialise Mimics (Materialise, Leuven, Belgium) for the export of the 3D models into the Materialise Mimics Viewing environment.

2.2.3 Viewing Environments

Three different visualization environments were employed: the CTA scan displayed on a 2D screen, the 3D model displayed on a 2D screen, and the 3D model displayed as a 3D hologram using AR. An overview of the three viewing environments is illustrated in Figure 1. The CTA scan and corresponding MIP reconstructions were displayed utilizing Sectra IDS7 (Sectra AB, Linköping, Sweden), as used in standard clinical practice. Participants assessed the CTA images and the MIP reconstructions. The 3D model on a 2D screen was displayed using the Materialise Mimics Viewing environment. This environment showed the axial, sagittal, and coronal CTA slices alongside the 3D model. For 3D holographic visualization, the Microsoft HoloLens 2 (Microsoft, Redmond, WA, USA) was utilized as the AR Head Mounted Device (HMD). The Materialise Mimics Viewing environment was installed as an application on the HoloLens and used accordingly. For both the CTA scan and 3D model environment, measurement capabilities were available. For the 3D model environment and the 3D hologram using AR, rotating around and zooming in and out of the 3D model was possible for detailed examination. The HoloLens also enabled the user to walk around the hologram. Furthermore,

in both environments, the visibility of the perforator, RA muscle, and fat tissue could independently be switched on or off or set to transparent.

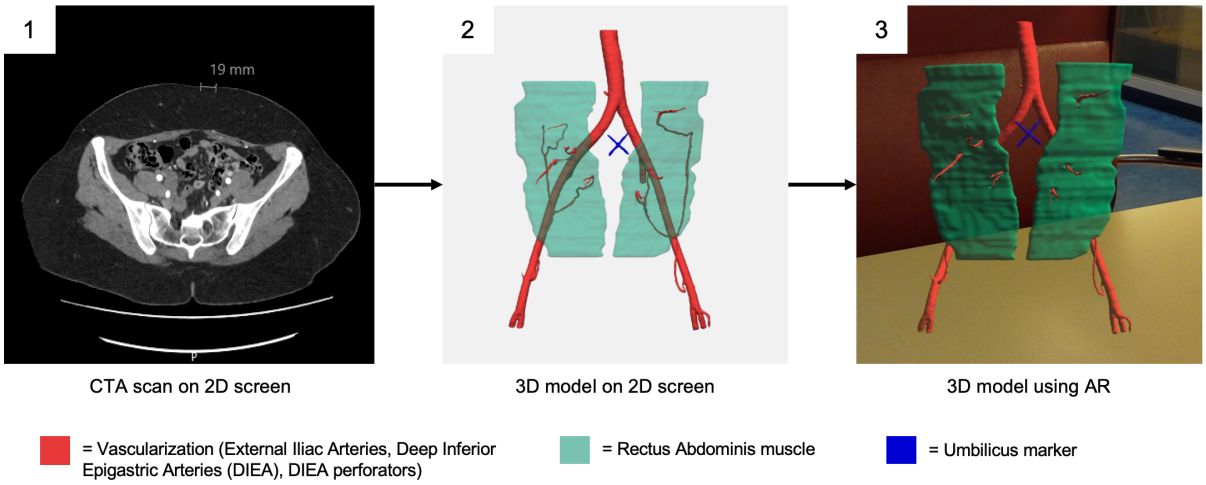

Figure 1. *The different viewing environments. (1) An axial slice of the conventional CTA scan on a 2D screen. (2) The 3D model on a 2D screen as presented in the Mimics viewer environment. (3) the 3D holographic visualization using Augmented Reality.*

2.3 Participants

Three surgeons from the plastic surgery department at LUMC participated in this study. One surgeon had 15-20 years of experience and performed approximately 15 DIEP flap surgeries annually, while the other two surgeons had 5-10 years of experience and performed around 20 DIEP flap surgeries annually.

2.4 Study Design

2.4.1 Test protocol

The participants examined the perforator anatomy of each patient in the three subsequent viewing environments, simulating a preoperative DIEP flap setting. A schematic overview of the test protocol can be seen in Figure 2. Participants were blinded to each other's results. To simulate clinical practice, the CTA scan on a 2D screen was first displayed. Participants assessed the CTA scan as they would in a preoperative setting and selected the optimal perforator. The optimal perforator indicates the perforator they would use intraoperatively. The perforator choice was documented in 3DSlicer by an independent observer. A perforator label was systematically assigned using a method depicted in Figure 3. 'R' or 'L' indicates the perforator's right or left branch, and numbers were assigned from medial to lateral, sequentially from the first perforator from the origin of the branch. Additionally, participants completed a questionnaire (chapter 2.4.2). Next, the 3D model on a 2D screen, followed by the 3D hologram using AR were examined. For each environment, participants identified the optimal perforator and completed the corresponding questionnaire. For patients who underwent DIEP flap reconstruction surgery during the period covered by the research described in the thesis, the perforator used intraoperatively was documented.

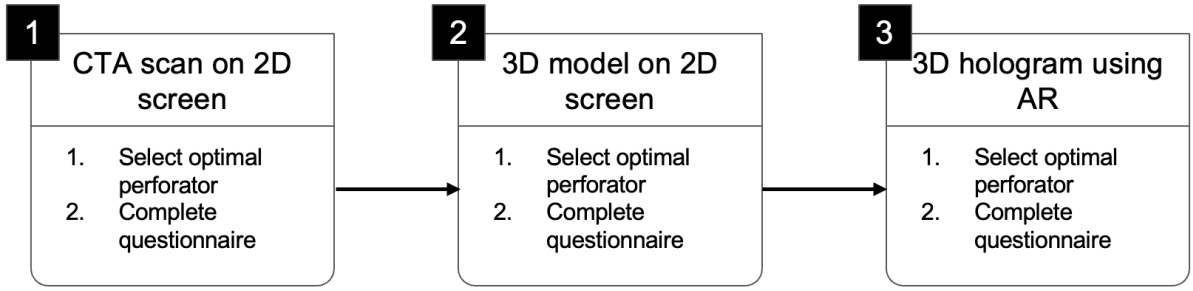

Figure 2. *A schematic overview of the test protocol, starting with the CTA scan on a 2D screen, followed by the 3D model on a 2D screen and the 3D hologram using Augmented Reality.*

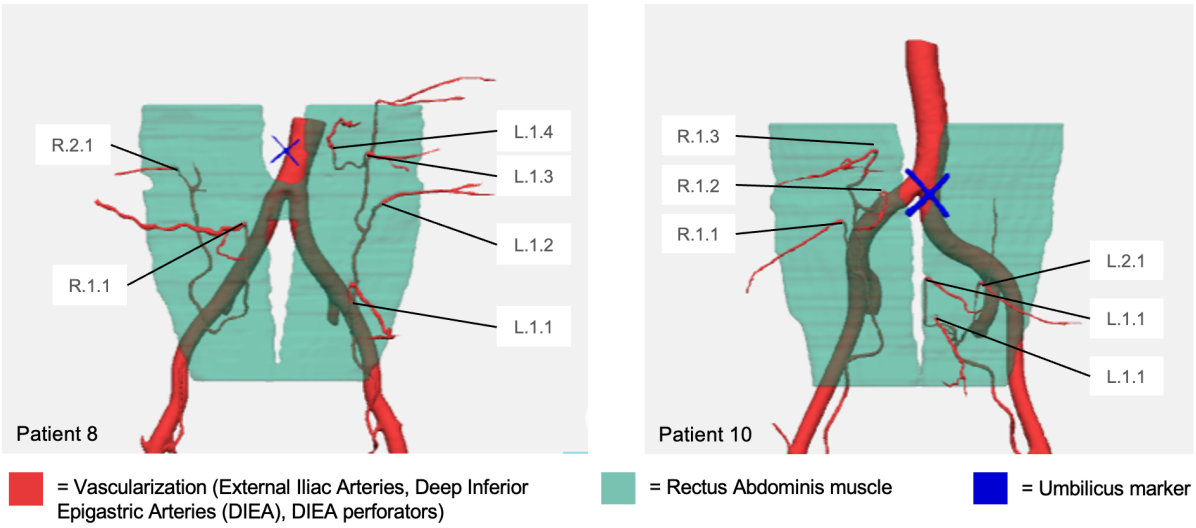

Figure 3. *The method for assigning the perforator label in two examples; 'R' or 'L' indicates the perforator's right or left branch, and numbers were assigned from medial to lateral, sequentially from the first perforator from the origin of the branch.*

2.4.2 Questionnaire

Participants completed a questionnaire after examining each viewing environment. The full questionnaire can be found in Appendix B. First, the visibility of the DIEP perforators was evaluated using the six key characteristics which are important in selecting the optimal perforator: calibre, intramuscular course, location in the flap, origin, subcutaneous branching pattern, and location relative to other vessels [24]. Participants rated how adequately they could assess each characteristic using a five-point Likert scale ranging from 'strongly disagree' to 'strongly agree'. Second, the characteristic(s) deemed most important in the selection of the optimal perforator were chosen, allowing for multiple answers. Furthermore, the confidence in using the selected perforator intraoperatively was evaluated. This assessment also employed a five-point Likert scale ranging from 'strongly disagree' to 'strongly agree'. For both the 3D model on a 2D screen and the 3D hologram using AR, an additional question was included to determine the surgeon's opinion on the implementation of the viewing environment in clinical practice. Comments and additional remarks were documented, categorized, and reviewed as supplementary information.

2.4.3 Statistical analysis

A descriptive analysis was performed using the Statistical Package for the Social Sciences (SPSS). The normality of the continuous data was tested using the Shapiro-Wilk test. Parametric variables were reported as mean ± standard deviation (SD), while non-parametric variables were reported as median (Mdn) with the interquartile range (IQR). For categorical variables, numbers and frequencies were reported. The differences between the viewing environments were tested for significance using the Friedman test and the Wilcoxon signed-rank test.

3. Results

A total of 15 patients were included in this study, Table 1 shows an overview of the demographics of the patients.

Table 1. *Patient demographics*

Parameter	
No. of patients	15
Unilateral reconstruction	13
Bilateral reconstruction	2
Number of flaps	17
Age (mean ± SD) (yr)	52 ± 8.0
BMI (mean ± SD) (kg/m^2)	30 ± 4.2

3.1 Perforator Choice

Each participant selected the optimal perforator for every patient in all three viewing environments. When utilizing the CTA scan on a 2D screen, variations in optimal perforator choice were observed for seven patients (47% of the patients). Complete disagreement, where each participant chose a different perforator, occurred for two patients. For the remaining five patients, partial disagreement was noted. For these patients, two participants selected the same perforator while the third chose a different one. After utilizing the 3D model on a 2D screen, the perforator choice changed seven times, reducing disagreement to two patients (13% of the patients). No further changes in optimal perforator selection were made after utilizing the AR environment. During the research period, four patients underwent the DIEP flap reconstruction surgery. When looking into the perforator choice from each participant, the optimal perforator choice in the CTA environment corresponded with the perforator used intraoperatively for nine out of the twelve choices (75%). This correspondence was eleven out of twelve (92%) for the perforator choice from the 3D model on the 2D screen. The optimal perforator choices are detailed in Table 2. Due to the absence of changes between the 3D model on a 2D screen and the AR environment, these results are not separately shown.

3.2 Questionnaire

3.2.1 Perforator Characteristics

Initial assessment of normality using the Shapiro-Wilk test indicated non-normal distributions (all p-values < 0.05). Consequently, medians and interquartile ranges (IQR) were reported. Figure 4 provides a detailed overview of the visibility scores for the different characteristics. The median and interquartile range (IQR) for calibre were 4 (3;4) for CTA on a 2D screen, 4 (4;5) for the 3D model on a 2D screen, and 5 (5;5) for the 3D hologram using AR. For the intramuscular course, the visibility scores were 4 (3;4), 5 (4;5), and 5 (5;5), respectively. The visibility scores for the perforator's location in the flap were 4 (3;4), 4 (4;5), and 5 (5;5). For the perforator origin, the scores were 4 (3;4), 5 (4;5), and 5 (5;5). The subcutaneous branching

pattern had scores of 4 (4;5), 4 (4;4), and 5 (4;5). Finally, the location relative to other vessels had visibility scores of 4 (4;5), 5 (4;5), and 5 (5;5). The Friedman test revealed significant differences in visibility scores across the three environments for all characteristics ($p < 0.001$).

Table 2. *Perforator choices per participant for every patient in the CTA scan and 3D model environment, and the intraoperatively used perforator.*

Patient	CTA scan on 2D screen			3D model on 2D screen			Intra-op
	1	2	3	1	2	3	
1	**R1.1***	L2.1	L2.1	L2.1	L2.1	L2.1	
2	R1.1/R1.2	L2.1/L2.2	L2.1/L2.2	L2.1/2.2	L2.1/2.2	L2.1/2.2	
3 (bilateral)	R1.1, L1.2	R1.1, L1.2	R1.1, L1.2	R1.1, L1.2	R1.1, L1.2	R1.1, L1.2	R1.1, L1.2
4	R1.1	R1.1	R1.1	R1.1	R1.1	R1.1	
5	L1.1	L1.1	**R1.1***	L1.1	L1.1	L1.1	
6 (bilateral)	L1.1/1.2, R1.2	**L2.1, R1.3***	L1.2, R1.2	L1.1/1.2, R1.2/1,3	L1.1/1.2, R1.3	L1.1/1.2, R1.2	
7	**L1.1/1.2***	**L2.1***	**R1.2/1.3***	L1.1/1.2	L1.1/1.2	**R1.2/1.3***	
8	R1.1	R1.1	R1.1	R1.1	R1.1	R1.1	
9	L1.1	L1.1	L1.1	L1.1	L1.1	L1.1	L1.1
10	R1.3	R1.3	R1.3	R1.3	R1.3	R1.3	
11	**L1.1 ***	**L2.2/2.1***	**R1.2***	**L1.1***	R1.2	R1.2	R1.2
12	L1.1	**R1.1***	L1.1	L1.1	L1.1	L1.1	
13	**L1.1/1.2***	R1.2	R1.2	R1.2	R1.2	R1.2	R1.2
14	L1.1	L1.1	L1.1	L1.1	L1.1	L1.1	
15	L1.1	L1.1	L1.1	L1.1	L1.1	L1.1	

**** =*** *Indicates a different choice from the other two participants or all participants chose differently*
/ = *Participant chose 2 perforators from the same branch, planning to use both intraoperatively*
, = *Indicating a bilateral reconstruction, an optimal perforator was chosen for both sides*
Due to the absence of changes between the 3D model on a 2D screen and the AR environment, these results are not separately shown.

Post-hoc pairwise comparisons using the Wilcoxon Signed-Rank Test with Bonferroni correction showed significant differences between all environments for each characteristic, except for the subcutaneous branching pattern between CTA on a 2D screen and the 3D model on a 2D screen ($p = 0.119$).

Participant feedback highlighted that 3D visualization was most beneficial for evaluating the intramuscular course, location in the flap, origin, and position relative to other vessels. The 3D model provided a clear initial overview of the anatomy, reducing the time required to interpret the anatomical structures. The AR environment best simulated the clinical setting, as it allowed surgeons to bring the patient's anatomy closer to their view, similar to operating with surgical loupes. A summarized overview of the comments and remarks is provided in Appendix C.

For the perforator characteristics considered most important in selecting the optimal perforator, calibre was most frequently selected, being employed in 82% of cases. Intramuscular course and location in the flap were used in 78% and 60% of cases, respectively. Table 3 provides an overview of the frequency with which each characteristic was considered important in the selection of the optimal perforator across different viewing

environments, cumulated for the three participants. The Shapiro-Wilk test indicated non-normal distributions in the number of characteristics considered for perforator choice across all viewing environments (all p-values < 0.05). The median number of characteristics considered was 3 (IQR: 2-3) for all three environments. The Friedman test showed no significant difference in the number of characteristics considered among the three environments (p = 0.092).

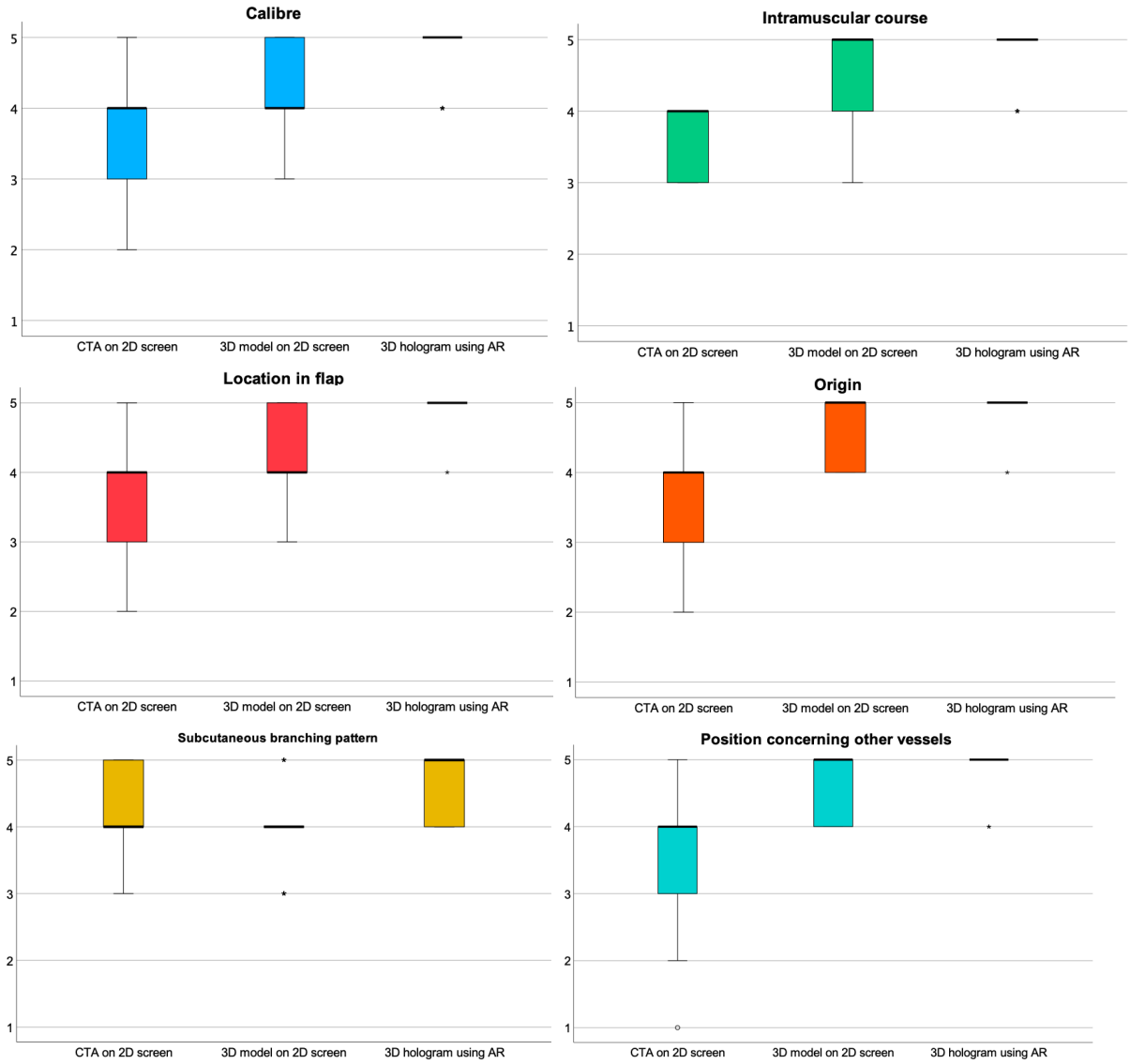

Figure 4. *The box plots showing the data distribution of the visibility scores for the six perforator characteristics given the median value and quartiles.*
Y-axis: Likert score (1-5), 5 indicating the best visibility. X-axis: the three different viewing environments.
****** in the graphs indicate outliers in the data.*

Table 4. *The number of times a characteristic was considered an important characteristic in the selection of the optimal perforator for the different viewing environments, combining the results from the three participants.*

	CTA scan	***3D model on 2D screen***	***3D hologram using AR***
Calibre	37	34	40
Intramuscular course	31	34	36
Location in flap	27	26	28
Origin	1	5	3
Subcutaneous branching pattern	9	6	9
Location compared to eachother	11	10	12
Total	116	115	128

3.2.2 Confidence level

Initial assessments of normality using the Shapiro-Wilk test indicated non-normal distributions (all p-values < 0.05). Figure 5 shows the overview of the confidence scores in perforator choice for the different viewing environments. The median and interquartile range (IQR) were 4 (3;4) for the CTA scan on a 2D screen, 4 (4;5) for the 3D model on a 2D screen, and 5 (5;5) for the 3D hologram using AR.

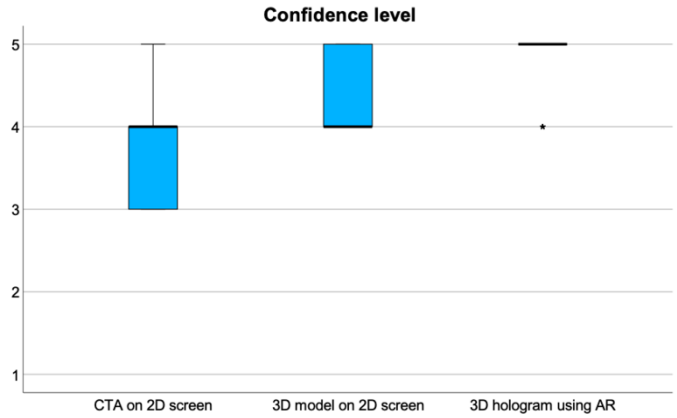

Figure 5. *The box plots visualizing the data distribution of the confidence scores in perforator selection given the median value and quartiles.*
Y-axis: Likert score (1-5), 5 indicating being most confident. X-axis: the three different viewing environments
** in the graphs indicate outliers in the data*

3.2.3 Future use

All participants reported that the 3D model on a 2D screen improved the preoperative planning of the DIEP flap compared to the conventional CTA scan, and preferred its use in clinical practice. The usage of the 3D model alongside the CTA scan was preferred 22 times (49%), while the usage of the 3D model alone was preferred 23 times (51%). Regarding the AR environment, all participants agreed that it further enhanced preoperative planning beyond both the CTA scan and the 3D model on a 2D screen, and expressed a preference for its clinical implementation. The preference for using the AR environment alongside the CTA scan was 21 times (47%), while the preference for using it exclusively was 24 times (53%).

4. Discussion

4.1 Interpretation of results

This study evaluated the added value and clinical potential of 3D visualization of DIEP flap perforator anatomy by comparing the conventional 2D CTA scan visualization with a 3D model on a 2D screen, and a 3D hologram using AR. The findings demonstrated that both the 3D model and 3D hologram improved the preoperative perforator visualization compared to the conventional CTA scan, with the AR-based 3D hologram showing the most significant improvement and being the most preferred technique. These results align with previous literature, demonstrating that 3D visualization significantly enhances the visualization of relevant anatomical structures and improves the surgeon's understanding of perforator anatomy [11], [17], [22], [48]. By integrating the visibility of perforator characteristics as an outcome, this study presented a consistent and reproducible method for demonstrating the impact of viewing environments on visualization. This approach can be utilized in future research when comparing new visualization techniques. Additionally, it not only identified the benefits of 3D visualization but also highlighted the preference for the AR-based method.

The integration of 3D visualization enhanced the consensus among surgeons regarding optimal perforator selection, increasing from 53% in the CTA environment to 87% in both the 3D model and AR environments. The concordance between preoperative and intraoperative perforator choices improved from 75% to 92%. These outcomes suggest more consistent decision-making and support more informed preoperative planning when utilizing 3D visualization techniques. Discrepancies in perforator choice in the CTA scan environment may be due to the 'slab' interpretation of MIP reconstructions, leading to inaccurate estimations of perforator position, origin, and course due to the loss of original spatial context [38]. In contrast, the 3D models, developed from original CTA data, provided enhanced visualization while maintaining accurate perforator locations and paths.

This study highlighted that 3D visualization improved the visibility of perforator characteristics, particularly the intramuscular course and anatomical relationships, such as perforator location within the flap, origin, and positions relative to other vessels. Participants noted that intramuscular dissection is one of the most technically challenging aspects of the DIEP flap procedure, emphasizing the enhanced understanding of the intramuscular course achieved through 3D visualization. In comparison with other preoperative planning techniques, a study by Chae et al. [41] proposed a 3D-printed template for preoperative perforator planning but found it inadequate for visualizing the intramuscular course.

Analyzing the frequency with which characteristics were considered in selecting the optimal perforator showed that the characteristics most enhanced by the 3D visualization were also the most frequently considered. Calibre was the most frequently considered characteristic. Although 3D visualization showed increased visibility for calibre, there were concerns about its validity in the 3D model.

Although AR did not further influence the outcomes of perforator choice, it showed the highest visibility scores and was the most preferred technique. One surgeon noted that the AR functionality, which allows bringing the 3D hologram closer to the eyes, effectively simulates the use of surgical loupes. The enhanced visibility and clinical resemblance increased

confidence in perforator choice and surgical approach, likely leading to better surgical outcomes and reduced operative times.

4.2 Strengths and limitations

This study's strengths include a comprehensive comparison of two 3D visualization environments against the conventional CTA scan on a 2D screen, showing the advancements of the 3D visualization and highlighting the outstanding of the 3D hologram using AR. The study included 15 patients, allowing the evaluation of multiple anatomical variations and enhancing the generalizability of findings. The inclusion of surgeons with varying experience levels further supports the robustness of the results.

However, there are also limitations. There was a consistent approach of showing the CTA scan on a 2D screen first, followed by the assessment of the other two environments. This test setup aimed to replicate future clinical practice, but may have introduced a learning bias as participants likely transferred information from the CTA scan to subsequent environments. Additionally, the semi-automated creation of 3D models was time-consuming and user-dependent. Potential human segmentation errors were directly translated into the experiment. The small sample size for evaluating the agreement between the preoperative selected and intraoperative used perforators limits the generalizability of the findings and underscores the need for further research with larger cohorts to validate these results. Additionally, no particular surgeon was designated as the gold standard for perforator selection; instead, the perforator chosen by the majority was deemed the correct choice. Future studies should consider designating one surgeon as the gold standard to enable more accurate comparisons.

4.3 Future perspectives

Future research should include cost-utility analyses to assess the economic feasibility of AR technology for DIEP flap reconstructions. Automating the segmentation process is crucial for improving cost-effectiveness and robustness. A study by Moens et al. [41] reported the first application of Deep Learning (DL) for automated perforator segmentation in DIEP flap breast reconstruction. The study demonstrated that DL has the potential to enhance the efficiency and objectivity of identifying DIEP vessels in CTA images. However, it revealed that the automated segmentations had only moderate agreement with manual segmentations and that the automatically developed model missed some perforators. This indicates that the DL algorithm requires further refinement before it can be used in clinical practice. To further enhance the 3D model, the possibility of automatically calculating the perforator caliber and caudal/cranial and lateral distance relative to the umbilicus could be investigated.

Before clinical implementation, the anatomical fidelity of the 3D models and the usability of AR devices should be tested. Following validation, the functionality of AR for overlaying the 3D hologram onto the patient should be developed and tested. This enables the integration of preoperative planning with real-time patient anatomy. To achieve this, a clinically viable registration technique must be created and evaluated, ensuring accuracy within the clinically acceptable 1 cm planning margin.

5. Conclusion

This study demonstrated the advantages of 3D visualization in the preoperative planning of DIEP flap breast reconstructions. Comparing the 3D model on a 2D screen with the 3D

hologram using AR revealed that AR offers superior visualization and is preferred for clinical practice. The enhanced visibility of perforator characteristics, improved consensus among surgeons, and increased confidence in perforator choice highlighted the potential of AR to improve the preoperative decision-making process, intraoperative approach, and surgical efficiency. Future efforts should focus on validating the 3D holograms using AR and testing the usability of the AR device. Future advancements in automated segmentation are expected to further enhance the utility of 3D visualization in clinical practice.

Chapter 4: The clinical validation and usability of Augmented Reality in DIEP flap breast reconstruction; a pilot study

1. Introduction

The Deep Inferior Epigastric Perforator (DIEP) flap is the preferred flap of choice for free flap breast reconstruction [9]. The DIEP flap utilizes the abdominal skin and fat tissue while preserving the rectus abdominis (RA) muscle and its nerves [8]. The correct identification and dissection of the Deep Inferior Epigastric Artery (DIEA) and its perforator vessels is essential for flap viability and diminishing postoperative fat necrosis [10], [11]. One or more dominant perforator vessels are identified and dissected along their intramuscular course, ensuring adequate pedicle length while preserving muscle functionality and minimizing donor site morbidity [12].

A preoperative understanding of the highly variable vascular anatomy of the DIEP flap aids in predicting the optimal perforator. Perforator characteristics considered in selecting the optimal perforator include the location of the perforator in the flap, calibre, intramuscular course through the RA muscle, perforator origin, subcutaneous branching pattern, and the position concerning other vessels [13]. Preoperative selection of the optimal perforator reduces operative time and postoperative complications while increasing the surgeon's confidence. Furthermore, it reduces the risk of inadvertent perforator selection or switching to an alternative flap type during surgery [14].

Imaging techniques such as computed tomographic angiography (CTA), magnetic resonance angiography (MRA), and Doppler ultrasonography (Doppler US) are preoperatively performed to assist in visualizing and identifying the optimal perforator. Although these methods effectively identify suitable perforators, they are limited by their 2D representation, necessitating surgeons to mentally reconstruct a 3D map of the vascular structures and their intramuscular course. This may result in uncertainty in identifying the optimal perforator and a suboptimal spatial understanding of the entire course of the perforator [15].

The incorporation of 3D visualization enhances surgeons' proficiency in tracking vascular pathways, assessing spatial relationships among anatomical landmarks, and evaluating vascular courses [11], [22]. The phase 1 study demonstrated the potential of Augmented Reality (AR) by improving the visibility of perforator characteristics, achieving consensus among surgeons on optimal perforator selection, and increasing confidence in this choice. This enhancement may further influence the preoperative decision-making processes, including flap type selection and operative approach. The HoloLens 2 is currently regarded as one of the most suitable AR devices for surgical practice [43], [44]. However, before clinical implementation, it is crucial to assess the viability of the 3D holograms and the device's usability. This pilot study aims to validate the 3D holograms of DIEP flap perforator anatomy using the HoloLens 2 by comparing them with intraoperative patient anatomy. Additionally, it evaluates surgeons' user experience and satisfaction with the device.

2. Method

2.1 Patients

Patients who underwent single or double autologous breast reconstruction using a DIEP flap at the Leiden University Medical Center (LUMC) between May 2024 and July 2024 were included.

2.2 Imaging Pipeline

2.2.1 Imaging

Routinely acquired CTA scans for the preoperative planning of DIEP flap reconstructions were utilized. The scans were acquired with either a Canon Aquilion ONE PRISM edition or a Canon Aquilion ONE GENESIS edition (slice thickness 0.5-1.0 mm, pixel spacing 0.782-1.949 mm, 100 kVp, tube current 83-425 mA, exposure time 500 ms). Maximum Intensity Projection (MIP) reconstructions with a slab thickness of 5 mm in axial, sagittal, and coronal were available.

2.2.2 3D Model Development

Patient-specific 3D models of the perforator anatomy, RA muscle, and fat tissue were created for each patient by one researcher. To account for the learning curve, the first 5 segmentations were checked by a plastic surgeon. Raw DICOM data of the preoperative CTA scan was uploaded into the image processing software 3DSlicer (v.5.0.3, Surgical Planning Laboratory, Brigham and Women's Hospital, Boston, MA, USA) for segmentation of the structures. The vascularization, RA muscle, and fat tissue were initially segmented using 'thresholding'. The threshold value was based on the trade-off between correctly segmenting the tissue of interest and diminishing noise. The segmentations were manually corrected by the researcher. Due to low contrast within the fat tissue, the subcutaneous vascular branching pattern was not included in the initial segmentation but was manually segmented. When in doubt about the presence of a perforator, the Maximum Intensity Projection (MIP) scan was used for verification. The model was checked against the radiology report to ensure that all optimal perforators identified in the report were at least segmented. The segmentations were exported as STL files and imported into the 3D modeling software Materialise Mimics (Materialise, Leuven, Belgium) for the export of the 3D models into the Materialise Mimics Viewing environment.

2.2.3 Viewing Environments

For the AR visualization of the patient-specific 3D models, the Microsoft HoloLens 2 (Microsoft, Redmond, WA, USA) was utilized. The Materialise Mimics Viewing environment was installed as an XR application on the HoloLens and used accordingly.

2.3 Participants

Three surgeons from the plastic surgery department at LUMC participated in this study. One surgeon had 15-20 years of experience and performed approximately 15 DIEP flap surgeries annually, while the other two surgeons had 5-10 years of experience and performed around 20 DIEP flap surgeries annually.

2.4 Study Design

2.4.1 Test Protocol

Participants prepared and performed the DIEP-flap surgery following clinical standards. The preoperative assessment included analyzing the patient's anatomy using a CTA scan

displayed on a 2D screen to select the optimal perforator for intraoperative use, subsequently marking its location on the patient's abdomen with a handheld Doppler. The Doppler search was guided by perforator location coordinates from the radiology report. The surgery was performed as in clinical practice. Postoperatively, participants used the HoloLens to visualize the 3D hologram, identified the optimal perforator based on the 3D hologram, and completed a questionnaire (chapter 2.4.2).

The optimal perforator was documented for the CTA scan, intraoperative used perforator, and the 3D hologram using the 3D model. Locations were recorded using a coordinate system with the umbilicus as the reference point (U-P), measured in lateral and caudal/cranial distances (cm). For the CTA scan, perforator locations from the radiology report were used. Coordinates were measured in Sectra IDS7 (Sectra AB, Linköping, Sweden) from a marker placed on the umbilicus to the fascia penetration point at skin level. The U-P measurements for the patient marking(s) were preoperatively measured at skin level. The intraoperative and 3D hologram U-P measurements were taken at the rectus sheath level. For the 3D hologram, these measurements were performed on the 3D model in 3DSlicer. Perforators suitable for supplying a flap were counted on the CTA scan, intraoperatively during flap elevation, and on the 3D hologram. Figure 1 shows a schematic overview of the test protocol. Figure 2 illustrates the 4 different measurement environments.

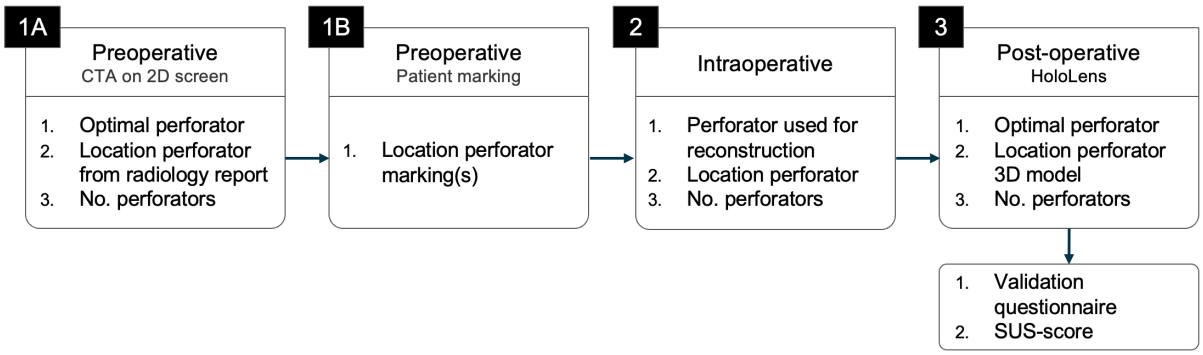

Figure 1. *The test protocol and parameters were documented for the preoperative, intraoperative, and postoperative situations.*

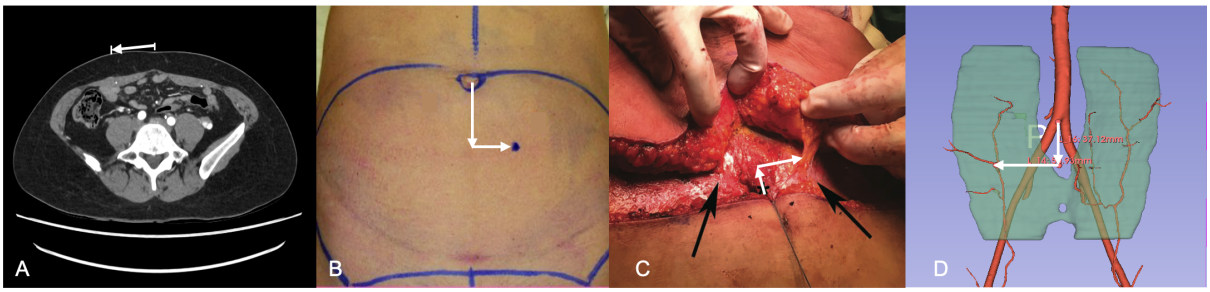

Figure 2. *Perforator location measurement in 4 environments; A) The CTA scan, B) the preoperative marking C) the intraoperative situation, and D) the 3D model, which is used as the 3D hologram in the HoloLens.*
**Images do not all show the same patient.*

An independent observer documented the data. Each perforator was labeled according to the method in Figure 3, with 'R' or 'L' indicating the right or left branch, and numbers assigned sequentially from medial to lateral, starting from the first perforator at the branch origin.

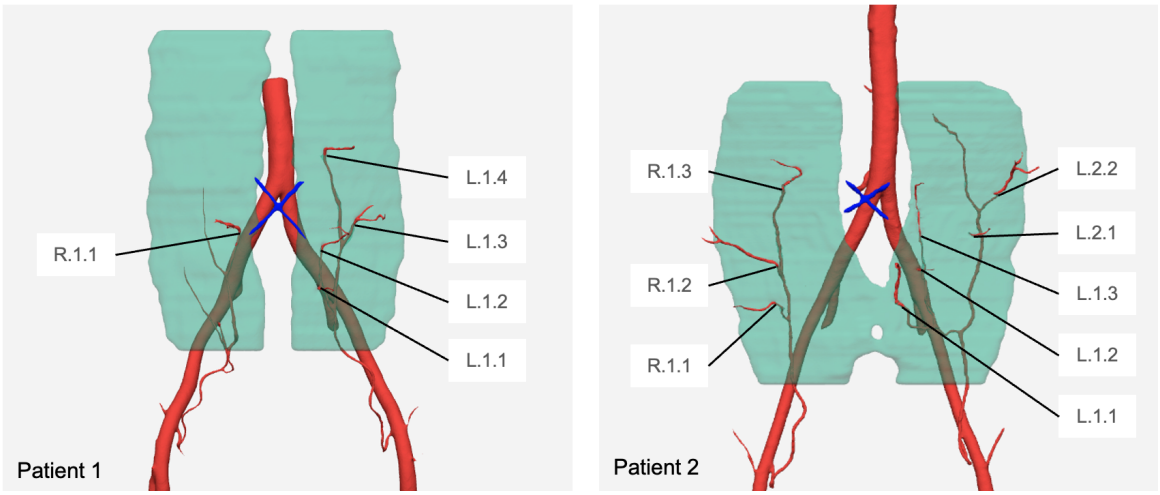

Figure 3. *The method for numbering the perforators for two example patients; 'R' or 'L' indicates the perforator's right or left branch, numbers were assigned from medial to lateral, sequentially from the first perforator from the origin of the branch.*

2.4.2 Questionnaire

Participants completed a questionnaire after examining the 3D hologram in the AR viewing environment. The full questionnaire is available in Appendix D and includes two components. First, the correspondence in the optimal perforator anatomy between intraoperatively assessed perforator anatomy and the 3D hologram was evaluated using five key perforator characteristics: calibre, intramuscular course, location in the flap, origin, and location relative to other vessels [24]. The subcutaneous branching pattern was not assessed because this characteristic was not intraoperatively visible. Participants rated the adequacy of the hologram's perforator characteristics in matching the patient anatomy on a five-point Likert scale ranging from 'strongly disagree' to 'strongly agree.' Furthermore, they rated to which extent they would like to use AR in the preoperative setting in the future, utilizing a similar Likert scale.

The second part assessed the usability of the HoloLens using the System Usability Scale (SUS). This scale is the most widely used standardized questionnaire for the assessment of perceived usability [45]. The 10-question scale is scored on a 5-point Likert scale ranging from 'strongly agree' to 'strongly disagree'. The final score for the SUS ranges from 0 to 100, where a higher score indicates better usability [46]. The article from Bangor et al. [46] was used to interpret the overall usefulness score.

2.4.3 Margin of Error

The margin of error (MOE) was calculated to validate the locations of the perforators. The preoperative coordinates from the CTA scan, the 3D hologram, and preoperative markings were compared with the intraoperative perforator locations. The Euclidean distance was calculated for each pair of preoperative and intraoperative perforator locations to determine the error in localization. The Euclidean distance *d* for each perforator was computed using the formula:

$$d = \sqrt{(x1 - x2)^2 + (y1 - y2)^2}$$

Where (x1, y1) represents the preoperative coordinates, and (x2, y2) represents the intraoperative coordinates. The MOE was calculated as the average Euclidean distance for each preoperative method.

$$MOE = \frac{\sum d}{n}$$

3. Results

A total of three patients were included in this pilot study, Table 1 shows the demographics of these patients.

Table 1. *Patient demographics*

Parameter	
No. of patients	3
Unilateral reconstruction	3
Bilateral reconstruction	0
Number of flaps	3
Age (mean ± SD) (yr)	51 ± 4.1
BMI (mean ± SD) (kg/m^2)	26 ± 2.0

3.1 Perforator Choice

Each participant selected the optimal perforator for every patient using both the CTA scan on a 2D screen and the AR environment with the HoloLens. For patients 1 and 2, who were also included in the phase 1 study, the optimal perforator selected in the AR environment in this study was used to minimize the influence of intraoperative knowledge on perforator choice. The perforator choices and the intraoperatively used perforator are shown in Table 2. The optimal perforator choice in the CTA environment corresponded with the intraoperatively used perforator for one patient. For patient 1, two perforators were preoperatively selected and marked on the patient. The perforator ultimately used intraoperatively was not the first encountered during surgery. The optimal perforator choice in the AR environment corresponded with the intraoperatively used perforator for all patients.

Table 2. *Perforator choices per patient for the two viewing environments and the intraoperatively used perforator.*

Patient	CTA scan on 2D screen	3D hologram with HoloLens	Intraoperative
1	L1.1/1.2, or R1.2	R1.2	R1.2
2	L1.1	R1.2	R1.2
3	L1.2	L1.2	L1.2

/ = Participant chose 2 perforators from the same branch, planning to both use intraoperatively

3.2 Perforator Number

All of the identified perforators on the CTA scan and the 3D hologram were confirmed intraoperatively.

Table 3. *The number of perforators counted using the CTA scan, Augmented Reality, and intraoperatively.*

Patient	CTA scan	AR	Intraoperative
1	5	5	5
2	6	6	6
3	4	4	4

3.3 Questionnaire

3.3.1 Characteristic validation

Table 4 shows the correspondence scores in the optimal perforator anatomy between intraoperatively assessed perforator anatomy and the 3D hologram for the different perforator characteristics. Calibre scored a mean of 4, intramuscular course 4, location in the flap 4.3, origin 4.7, and location relative to other vessels 4.

Table 4. *Scores for the optimal perforator anatomy correspondence between intraoperatively assessed perforator anatomy and the 3D hologram.*

	Patient 1	Patient 2	Patient 3
Calibre	5	3	4
Intramusculair course	5	3	4
Location in the flap	4	4	5
Origin	5	4	5
Location relative to other vessels	4	4	4

**Score based on Likert scale (1-5), 5 indicating the best correspondence*

3.3.2 Future use

For all patients, the participants indicated that they would like to use AR in the preoperative setting. They assigned the highest score of ‘strongly agree’ in all cases.

3.3.3 SUS-score

The usability, as measured by SUS-score, resulted in scores of 77.5, 100, and 72.5. The mean score was 83.33 ± 12.0 (mean ± SD), indicating an "excellent" level of usability [45].

3.4 Margin of Error

The lateral and caudal locations of the optimal perforators for the different environments can be found in Table 5. One perforator intraoperatively used was not preoperatively marked on the patient’s skin. For two perforators, the intraoperative locations could not be measured. Compared with intraoperative locations, the average MOE for perforator localization was 0.8 cm ± 0.2 (mean ± SD) for the radiology report, 0.2 cm ± 0.2 for the 3D model, and 2.8 cm ± 1.3 for the preoperative marking. Figure 4 gives an overview of the MOE and Standard Deviation.

Table 5. *Perforator locations with the umbilicus as a reference point (U-P), shown as x, y (lateral, caudal), in (cm).*

Patient	Perforator	Radiology report	3D model	Preoperative marking	Intraoperative location
1	L1.1	3.1, 5.0	2.5, 4.7	3.3, 6.0	2.1, 4.8
	L1.2	2.6, 2.3	2.8, 2.0	3.3, 2.3	x
	R1.2	2.6, 1.5	2.1, 1.5	3.7, 0.0	2.0, 1.3
2	L1.1	0.8, 5.2	0.8, 5.4	3.5, 4.0	x
	R1.2	5.5, 3.3	5.1, 3.7	x	5.0, 3.9
3	L1.2	0.9, 7.7	1.0, 7.0	4.5, 4.0	1.0, 7.0

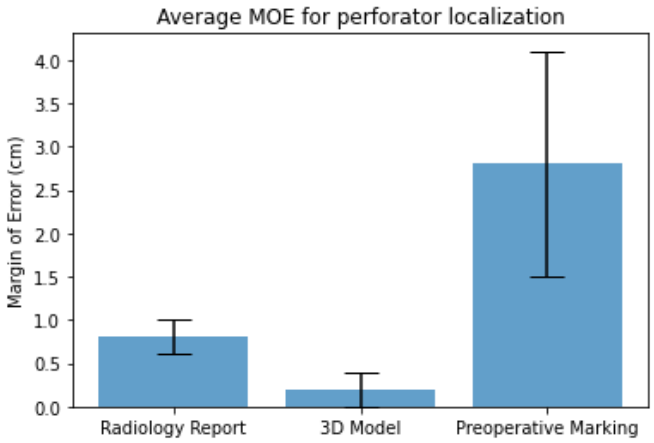

Figure 3. *The average MOE for perforator localization compared to the intraoperative findings.*

4. Discussion

4.1 Interpretation of results

This pilot study aimed to validate the 3D holograms of DIEP flap optimal perforator anatomy using the HoloLens 2 by comparing them with intraoperative patient anatomy, while also evaluating the surgeons' user experience with this device. The results demonstrated a high correspondence between the optimal perforator anatomy of the 3D hologram and intraoperative findings, as well as improved perforator selection agreement. The usability of the HoloLens was rated as excellent, and participants expressed a strong preference for using AR in preoperative planning.

The concordance between the preoperatively selected perforator using AR and the intraoperatively used perforator was 100%, compared to 67% with the CTA scan on a 2D screen. This indicates a potentially more consistent decision-making process in identifying the optimal perforator. All intraoperatively identified perforators were also detected on both the 3D hologram and the CTA scan. This aligns with previous studies demonstrating the high accuracy of CTA in detecting perforators, with sensitivity rates ranging from 90% to 100% [30], [47].

All perforator characteristics achieved a minimum score of 4 for intraoperative correspondence, indicating that the 3D hologram adequately matched the patient's anatomy for the optimal perforator. The margin of error (MOE) for perforator coordinates from the radiology report and the 3D model were 0.8 cm and 0.2 cm, respectively. Defazio et al. documented MOEs ranging from 0.5 to 0.7 cm for conventional CTA scans, supporting our findings. The larger error in preoperative marking (2.3 cm) underscores the limitations of using the handheld Doppler for perforator localization. The preoperative markings exceeded the clinically acceptable MOE of 1 cm for perforator localization in all three patients, highlighting the potential benefits of introducing augmented reality (AR) [30].

4.2 Strengths and limitations

This study's strengths include a comprehensive validation of 3D holograms using correspondence scores, MOE, and surgeon feedback. The utilization of the SUS-score adds robustness to the usability findings. Integrating perforator characteristics into the 3D model validation introduced a consistent and reproducible method.

However, this study has some limitations. The sample size is small, with only three patients included, limiting the generalizability of the results. Additionally, one perforator used intraoperatively was not preoperatively marked on the patient's skin, and for two perforators, intraoperative locations could not be measured due to practical constraints. These factors introduce variability and potential bias in the results. Furthermore, the semi-automated development of the 3D models may introduce human error, diminishing the 3D models' correctness. Future studies should aim to refine and automate the segmentation process to enhance accuracy and efficiency.

4.3 Future perspectives

Future research should focus on expanding the sample size to validate these findings across a more extensive and diverse patient population. Furthermore, displaying the 3D hologram preoperatively would add significant value. Preoperative visualization simulates the AR integration into the clinical workflow more closely, thereby increasing the applicability of the results. This approach enables the assessment of the surgeon's evaluation of the optimal perforator anatomy from the 3D hologram without the influence of intraoperative information. Additionally, it ensures that perforator selection is based solely on preoperative data rather than information obtained during surgery.

Furthermore, a clinical workflow for the registration of the 3D hologram with the patient should be developed and tested. This direct overlay facilitates the translation of the preoperatively selected perforator location to the patient, potentially increasing the accuracy of preoperative perforator marking and reducing pre- and intraoperative times and complications. The proposed registration technique should be practically implementable and have an error margin within the clinically acceptable range of 1 cm.

5. Conclusion

In conclusion, this pilot study demonstrated the promise of AR, specifically using the HoloLens 2, in enhancing preoperative planning for DIEP flap reconstructions. By validating the high correspondence between the optimal perforator anatomy in 3D holograms and intraoperative findings, along with positive surgeon feedback, this study contributes to the ongoing advancement of AR in clinical practice. Future research should focus on expanding the sample size to validate these findings across a more extensive and diverse patient population. With additional research and refinement, AR can become a vital tool in DIEP flap reconstruction planning, enhancing both outcomes and efficiency.

References

[1] Smolarz B, Nowak AZ, Romanowicz H. Breast cancer—epidemiology, classification, pathogenesis and treatment (review of literature). Cancers. 2022;14(10):2569.
[2] Sung H, Ferlay J, Siegel RL, Laversanne M, Soerjomataram I, Jemal A, et al. Global cancer statistics 2020: GLOBOCAN estimates of incidence and mortality worldwide for 36 cancers in 185 countries. CA: a cancer journal for clinicians. 2021;71(3):209-49.
[3] Boughey JC, Attai DJ, Chen SL, Cody HS, Dietz JR, Feldman SM, et al. Contralateral prophylactic mastectomy (CPM) consensus statement from the American Society of Breast Surgeons: data on CPM outcomes and risks. Annals of surgical oncology. 2016;23:3100-5.
[4] Ng SK, Hare RM, Kuang RJ, Smith KM, Brown BJ, Hunter-Smith DJ. Breast reconstruction post mastectomy: patient satisfaction and decision making. Annals of plastic surgery. 2016;76(6):640-4.
[5] Howard-McNatt MM. Patients opting for breast reconstruction following mastectomy: an analysis of uptake rates and benefit. Breast Cancer: Targets and Therapy. 2013:9-15.
[6] Toyserkani NM, Jørgensen MG, Tabatabaeifar S, Damsgaard T, Sørensen JA. Autologous versus implant-based breast reconstruction: A systematic review and meta-analysis of Breast-Q patient-reported outcomes. Journal of Plastic, Reconstructive & Aesthetic Surgery. 2020;73(2):278-85.
[7] Saldanha IJ, Broyles JM, Adam GP, Cao W, Bhuma MR, Mehta S, et al. Autologous breast reconstruction after mastectomy for breast cancer: a systematic review. Plastic and Reconstructive Surgery Global Open. 2022;10(3).
[8] Garvey PB, Buchel EW, Pockaj BA, Casey III WJ, Gray RJ, Hernández JL, et al. DIEP and pedicled TRAM flaps: a comparison of outcomes. Plastic and reconstructive surgery. 2006;117(6):1711-9.
[9] Kiely J, Kumar M, Wade RG. The accuracy of different modalities of perforator mapping for unilateral DIEP flap breast reconstruction: a systematic review and meta-analysis. Journal of Plastic, Reconstructive & Aesthetic Surgery. 2021;74(5):945-56.
[10] Miranda BH, Pywell M, Floyd D. A preoperative marking template for deep inferior epigastric artery perforator flap perforators in breast reconstruction. Archives of Plastic Surgery. 2014;41(02):171-3.
[11] Galstyan A, Bunker MJ, Lobo F, Sims R, Inziello J, Stubbs J, et al. Applications of 3D printing in breast cancer management. 3D printing in medicine. 2021;7(1):1-10.
[12] Steenbeek LM, Peperkamp K, Ulrich DJ, Hummelink S. Alternative imaging technologies for perforator mapping in free flap breast reconstructive surgery–A comprehensive overview of the current literature. Journal of Plastic, Reconstructive & Aesthetic Surgery. 2022;75(11):4074-84.
[13] Thimmappa N, Bhat AP, Bishop K, Nagpal P, Prince MR, Saboo SS. Preoperative cross-sectional mapping for deep inferior epigastric and profunda artery perforator flaps. Cardiovascular Diagnosis and Therapy. 2019;9(Suppl 1).
[14] Lam D, Mitsumori L, Neligan P, Warren B, Shuman W, Dubinsky T. Pre-operative CT angiography and three-dimensional image post processing for deep inferior epigastric perforator flap breast reconstructive surgery. The British Journal of Radiology. 2012;85(1020).
[15] Jiang T, Yu D, Wang Y, Zan T, Wang S, Li Q. HoloLens-based vascular localization system: precision evaluation study with a three-dimensional printed model. Journal of medical Internet research. 2020;22(4).
[16] Aubry S, Pauchot J, Kastler A, Laurent O, Tropet Y, Runge M. Preoperative imaging in the planning of deep inferior epigastric artery perforator flap surgery. Skeletal radiology. 2013;42:319-27.
[17] Berger MF, Winter R, Tuca AC, Michelitsch B, Schenkenfelder B, Hartmann R, et al. Workflow assessment of an augmented reality application for planning of perforator flaps in plastic reconstructive surgery: Game or game changer? Digital Health. 2023;9:20552076231173554.

[18] Lungu AJ, Swinkels W, Claesen L, Tu P, Egger J, Chen X. A review on the applications of virtual reality, augmented reality and mixed reality in surgical simulation: an extension to different kinds of surgery. Expert review of medical devices. 2021;18(1):47-62.
[19] Rozen W, Ashton M, Stella D, Phillips T, Taylor G. Stereotactic image-guided navigation in the preoperative imaging of perforators for DIEP flap breast reconstruction. Microsurgery: Official Journal of the International Microsurgical Society and the European Federation of Societies for Microsurgery. 2008;28(6):417-23.
[20] Allen RJ, Treece P. Deep inferior epigastric perforator flap for breast reconstruction. Annals of plastic surgery. 1994;32(1):32-8.
[21] Pellegrin A, Belgrano M, Cova MA. Preoperative vascular mapping with multislice CT of deep inferior epigastric artery perforators in planning breast reconstruction after mastectomy. In: Breast Reconstruction: Art, Science, and New Clinical Techniques. Springer; 2013. p. 145-52.
[22] Rozen WM, Palmer KP, Suami H, Pan WR, Ashton MW, Corlett RJ, et al. The DIEA branching pattern and its relationship to perforators: the importance of preoperative computed tomographic angiography for DIEA perforator flaps. Plastic and reconstructive surgery. 2008;121(2):367-73.
[23] Boyd JB, Taylor GI, McCraw JB. The vascular territories of the superior epigastric and the deep inferior epigastric systems. Plastic and Reconstructive Surgery. 1984;73(1):15-6.
[24] Ireton JE, Lakhiani C, Saint-Cyr M. Vascular anatomy of the deep inferior epigastric artery perforator flap: a systematic review. Plastic and reconstructive surgery. 2014;134(5):810e-821e.
[25] Wong K, Stubbs E, McRae M. CTA in preoperative planning for DIEP breast reconstruction: what the reconstructive surgeon wants to know. A modified Delphi study. Clinical Radiology. 2019;74(12):973-e15.
[26] Kikuchi N, Murakami G, Kashiwa H, Homma K, Sato T, Ogino T. Morphometrical study of the arterial perforators of the deep inferior epigastric perforator flap. Surgical and Radiologic Anatomy. 2002;23:375-81.
[27] Hummelink S, Hameeteman M, Hoogeveen Y, Slump C, Ulrich D, Kool LS. Preliminary results using a newly developed projection method to visualize vascular anatomy prior to DIEP flap breast reconstruction. Journal of plastic, reconstructive & aesthetic surgery. 2015;68(3):390-4.
[28] Choi EMO, Ribeiro RDA, Montag E, Ueda T, Okada AY, Munhoz AM, et al. The Influence of the Superficial Venous System on DIEP Flap Drainage in Breast Reconstruction. Journal of Reconstructive Microsurgery. 2023.
[29] Rudolf Buntic M. The Deep Inferior Epigastric Artery perforator (DIEP) flap;. Available from: https://www.microsurgeon.org/diep.
[30] Cina A, Salgarello M, Barone-Adesi L, Rinaldi P, Bonomo L. Planning breast reconstruction with deep inferior epigastric artery perforating vessels: multidetector CT angiography versus color Doppler US. Radiology. 2010;255(3):979-87.
[31] Doughty M, Ghugre NR, Wright GA. Augmenting performance: A systematic review of optical see-through head-mounted displays in surgery. Journal of Imaging. 2022;8(7):203.
[32] Hummelink S, Hoogeveen YL, Kool LJS, Ulrich DJ. A new and innovative method of preoperatively planning and projecting vascular anatomy in DIEP flap breast reconstruction: a randomized controlled trial. Plastic and reconstructive surgery. 2019;143(6):1151e-1158e.
[33] Docs M. What is mixed reality? - Mixed Reality;. Available from: https://learn.microsoft.com/en-us/windows/mixed-reality/discover/mixed-reality.
[34] Furman AA, Hsu WK. Augmented reality (AR) in orthopedics: current applications and future directions. Current reviews in musculoskeletal medicine. 2021:1-9.
[35] Nunes JS, Almeida FB, Silva LS, Santos VM, Santos AA, de Senna V, et al. Three-dimensional coordinate calibration models for augmented reality applications in indoor industrial environments. Applied Sciences. 2023;13(23):12548.
[36] Docs M. About HoloLens 2;. Available from: https://learn.microsoft.com/en-

us/hololens/hololens2-hardware.
[37] Pollefeys M. Microsoft HoloLens facilitates computer vision research by providing access to raw image sensor streams with Research Mode;. Available from: https://www.microsoft.com/en us/research/blog/microsoft-hololens-facilitates-computer-vision-research-by-providing-access-to-raw-image-sensor-streams-with-research-mode/.
[38] DeFazio MV, Arribas EM, Ahmad FI, Le-Petross HT, Liu J, Chu CK, et al. Application of Three-Dimensional Printed Vascular Modeling as a Perioperative Guide to Perforator Mapping and Pedicle Dissection during Abdominal Flap Harvest for Breast Reconstruction. Journal of Reconstructive Microsurgery. 2020;36(05):325-38.
[39] Cody DD. AAPM/RSNA physics tutorial for residents: topics in CT: image processing in CT. Radiographics. 2002;22(5):1255-68.
[41] Moes I, Corten E, Van Walsum T. Segmentation of Deep Inferior Epigastric Artery Perforators for Breast Reconstruction using Deep Learning in Computed Tomography Angiography: A Quantitative and Qualitative Evaluation. http://resolver.tudelft.nl/uuid:663e8b5f-d860-4a71-b11d-4426e4ad8253
[42] Chae MP, Hunter-Smith DJ, Chung RD, Smith JA, Rozen WM. 3D-printed, patient-specific DIEP flap templates for preoperative planning in breast reconstruction: a prospective case series. Gland Surgery. 2021;10(7):2192.
[43] Gasques Rodrigues D, Jain A, Rick SR, Shangley L, Suresh P, Weibel N. Exploring mixed reality in specialized surgical environments. In: Proceedings of the 2017 CHI Conference Extended Abstracts on Human Factors in Computing Systems; 2017. p. 2591-8.
[44] Cui N, Kharel P, Gruev V. Augmented reality with Microsoft HoloLens holograms for near infrared fluorescence based image guided surgery. In: Molecular-guided surgery: molecules, devices, and applications III. vol. 10049. SPIE; 2017. p. 32-7.
[45] Lewis JR. The system usability scale: past, present, and future. International Journal of Human–Computer Interaction. 2018;34(7):577-90.
[46] Bangor A, Kortum PT, Miller JT. An empirical evaluation of the system usability scale. Intl Journal of Human–Computer Interaction. 2008;24(6):574-94.
[47] Rozen WM, Ashton MW, Stella DL, Phillips TJ, Taylor GI. The accuracy of computed tomographic angiography for mapping the perforators of the DIEA: a cadaveric study. Plastic and reconstructive surgery. 2008;122(2):363-9.
[48] Seth I, Lindhardt J, Jakobsen A, Thomsen JB, Kiil BJ, Rozen WM, et al. Improving Visualization of Intramuscular Perforator Course: Augmented Reality Headsets for DIEP Flap Breast Reconstruction. Plastic and Reconstructive Surgery–Global Open. 2023;11(9):e5282.

Appendix A – Literature Review

'The intraoperative application of post-processing techniques in DIEP flap breast reconstruction surgery: a comprehensive overview of current literature'

MH Eijssen [1*], RPJ van den Ende[2], PS Verduijn[3], AND RR Dijkman[3]

[1]*Student MSc Technical Medicine Imaging & Intervention [4666925]; Technical University of Delft, Leiden University Medical Center* [2]*Technical supervisor; Department of Oral and Maxillofacial Surgery, Leiden University Medical Center, The Netherlands*
[3]*Medical supervisor; Department of Plastic Surgery, Leiden University Medical Center, The Netherlands*

Master Literature Study (TM30002; 10 ECTs); MSc Technical Medicine Imaging Intervention

Introduction: Effective identification of the Deep Inferior Epigastric Artery (DIEA) and its perforator vessels is crucial in DIEP free flap surgery. Traditional imaging like CTA, MRA, and Doppler US assist in preoperative perforator mapping but lack 3D visualization and direct translation to the intra-operative field. this review aims to present a thorough assessment of techniques using post-processed volumetric data (CTA or MRA) for enhanced intra-operative perforator mapping in DIEP flap breast reconstruction.

Method: A systematic search was conducted on December 12th, 2023, using PubMed, Embase, Medline, and Scopus databases. Articles focusing on post-processing methodologies applied to volumetric datasets for intra-operative perforator navigation in DIEP flap surgery were included. The selection criteria emphasized articles presenting quantitative outcomes like accuracy metrics or operation time. Extracted study characteristics were the investigated technology, number of participants, outcomes, control methods, performance evaluation metrics, and corresponding results.

Results: Eight studies met the eligibility criteria and were included in the review. Augmented Reality, 3D-printed anatomical models, and templates were included as investigated techniques. Outcome measures ranged from accuracy, correctly identified perforators, pre- and intra-operative time, complications, and usability. The studies varied in their approach and outcomes but consistently showed the potential of these techniques in improving surgical outcomes and efficiency.

Conclusion: The review identified a growing interest in techniques using post-processed volumetric datasets for intra-operative perforator mapping in DIEP flap breast reconstruction. While various methods are explored, quantitative data on their effectiveness is limited. While AR emerged as the most promising method in perforator mapping, future research should focus on the usability and impact of AR on surgical outcomes in DIEP flap surgery.

Introduction

Breast cancer is the most prevalent malignant tumor among women globally [1]. This disease accounted for approximately 12% of all new cancer cases in 2020, affecting an estimated 7.8 million women worldwide [2]. Surgery is the main treatment option for breast cancer, typically involving either breast conservation surgery (BCS) or mastectomy. BCS involves removing the malignant tumor and a small margin of surrounding healthy tissue, while in mastectomy the complete breast is removed [3].

Women undergoing breast reconstruction after mastectomy show enhanced psychosocial and sexual well-being and improved quality of life, compared to those without subsequent reconstruction [4]. Reconstructive surgery options include either implant-based methodologies or autologous tissue transfer employing a free flap technique. This latter approach utilizes the patient's tissue and is associated with higher patient satisfaction compared to implant-based reconstructions [5], [6]. The most common tissue flaps for breast reconstruction are the rectus transversus abdominis musculocutaneous (TRAM) flap and the deep inferior epigastric perforator (DIEP) flap [7]. The TRAM flap involves removing all or part of the rectus abdominis muscle, while the DIEP flap uses only skin and fat tissue, preserving the muscle and its nerves [8]. The DIEP flap leads to fewer complications and a shorter hospital stay, making it the preferred choice for reconstruction [9].

In free flap surgery, the correct identification and dissection of the Deep Inferior Epigastric Artery (DIEA) and its perforator vessels is essential for flap viability and diminishing postoperative fat necrosis [10], [11]. One or more dominant perforator vessels are identified and dissected along their intramuscular course, ensuring adequate pedicle length while preserving muscle functionality and minimizing donor site morbidity [12]. Important characteristics in the selection of the dominant perforator are the location of the perforator in the flap, calibre, intramuscular course through the rectus abdominis, perforator origin, subcutaneous branching, and the position concerning other vessels [13]. A preoperative understanding of the highly variable vascular anatomy of the DIEP flap helps in predicting the optimal perforator. This reduces operative time and postoperative complications while increasing the surgeon's confidence. Additionally, it reduces the risk of unforeseen selection of a different perforator or switching to an alternative flap type during surgery [14].

Imaging techniques such as computed tomographic angiography (CTA), magnetic resonance angiography (MRA), and Doppler ultrasonography (Doppler US) are preoperatively performed to assist in visualizing and selecting the optimal perforator. Although these methods effectively identify suitable perforators, they are limited by a 2D representation and require the surgeon to mentally reconstruct a 3D map of the vascular structures and their intramuscular course. The incorporation of 3D visualization into DIEP flap surgery would enhance the surgeon's proficiency in tracking vascular pathways, assessing their proximity to each other and anatomical landmarks, and evaluating their course [11]. Furthermore, these techniques lack direct translation from the computer screen to the corresponding anatomical location on the patient and fail to provide an intraoperative visualization of the intramuscular course of the DIEP vascular tree [15].

Recent advancements in alternative techniques significantly improved the perforator visualization and translation of preoperative planning into surgery. A review by Steenbeek et al. [12] provides an overview of the application of these techniques. However, it only provides an initial overview of the techniques and lacks a comprehensive summary of details such as outcome metrics and the respective advantages and disadvantages of each technique. Additionally, since the publication of the article in 2021, new articles focusing on for example Augmented Reality (AR) have been published.

This review specifically focuses on techniques that employ post-processing volumetric datasets (CTA or MRA) for perforator mapping in DIEP flap breast reconstruction surgery. Mapping encompasses the visualization of the perforators and the translation of the

preoperative planning into the intraoperative situation. Techniques such as fluorescent angiography and dynamic infrared thermography are beyond the scope of this overview, as they do not rely on preoperative planning with volumetric data. This review aims to present a thorough assessment of the applications, quantitative outcomes, advantages, and limitations of the selected techniques, providing an overview of their efficacy and utility.

1. Methods

2.1 Search strategy

On the 12th of December 2023, a systematic search was conducted using the databases of PubMed, Embase, Medline, and Scopus. For transparency and reproducibility, the full electronic search strategy is provided in Appendix A. In addition, the reference lists of articles that were screened on full text were scanned to supplement the potential missing articles.

2.2 Study selection criteria

The titles and abstracts of these articles were screened for relevance based on the inclusion and exclusion criteria. Articles that elaborated on post-processing methodologies applied to volumetric datasets for intra-operative perforator navigation in DIEP flap reconstructive breast surgery were included. Additionally, articles were required to present quantitative outcomes, such as accuracy metrics or operation time. Articles describing non-human studies, not published in English, or of which no full text was available were excluded from this review. Subsequently, the remaining articles were assessed for eligibility based on full-text reading.

2.3 Outcome measures

Study characteristics were extracted using a data collection sheet, including author name, year of publication, study design, investigated technology, number of participants, outcomes, control methods/technology, performance evaluation metrics, and corresponding results.

2. Results

3.1 Search results

The literature search resulted in 794 articles, of which 431 were duplicates. 334 articles were excluded based on title and/or abstract. 6 articles were identified from bibliographic linkages. The full text of the resulting 35 articles was assessed. 27 articles were excluded based on the exclusion criteria, which are shown in Figure 1. As a result, 8 studies were included in this systematic literature study [16]-[23]. Figure 1 shows the PRISMA flow diagram for study selection.

3.2 Study characteristics

The articles included in the review were published between 2009 and 2023. Each article addressed a specific post-processing technique employed in DIEP flap breast reconstruction surgery. Four articles investigated the application of Augmented Reality (AR) [16]-[19], two articles used a 3D printed anatomical model [20], [21], and two articles described templates [22], [23]. The majority of the articles [17]–[23] conducted a comparative analysis of the investigated technique, measuring them against intra-operative findings or findings from CTA and/or Doppler US, which are known as the gold standard for perforator mapping in DIEP flap surgery [24]. One article [16] utilized MRA data for the development of the technique and comparative analysis. In all articles, the anatomical information of the planning was

preoperatively demarcated on the patient's skin. A more detailed overview of the characteristics of the included articles is presented in Table 1.

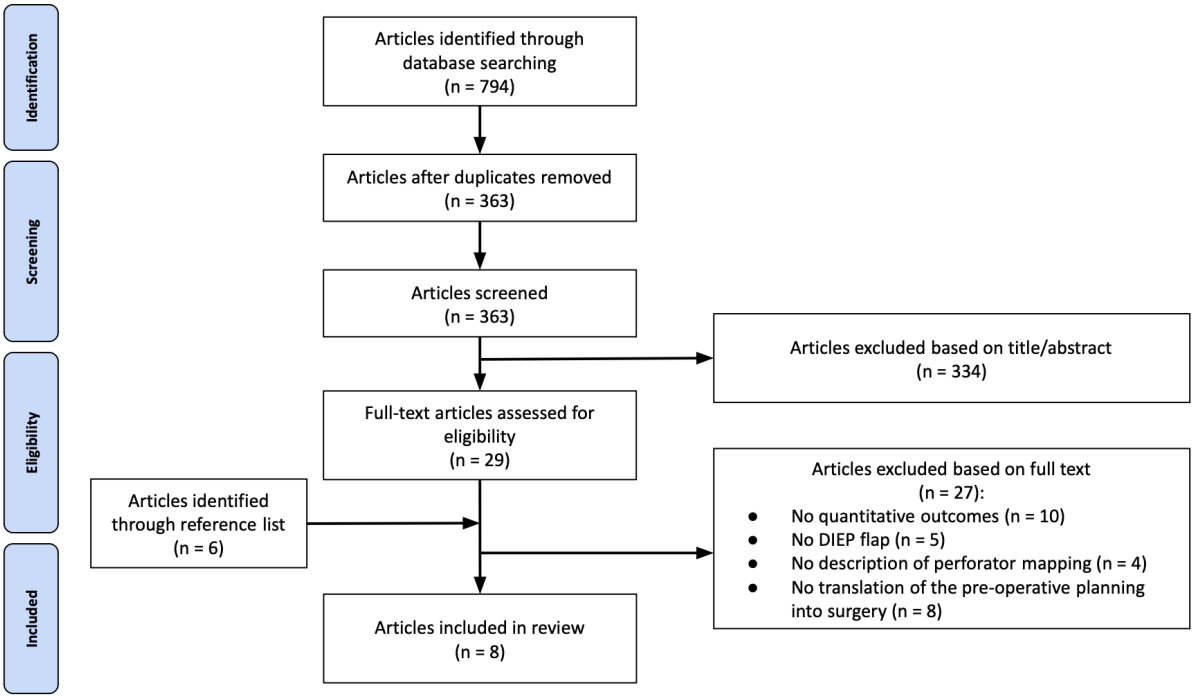

Figure 1 - PRISMA flow diagram of article selection

Table 1 - Primary study characteristics

Author	Technique	Study Design	Population size	Outcomes	Control method
Berger et al., 2023 [16]	AR HMD	Pilot study	n: 7	Accuracy, usability, workload	MRA
Fitoussi et al., 2021 [17]	AR VST	Feasibility study	n: 12	Accuracy	Doppler US
Hummelink et al., 2019 [18]	AR Projection	RCT	n: 60, Study group: 33, Control group: 27	Correctly identified perforators, operation time, complications	CTA and Doppler US
Hummelink et al., 2015 [19]	AR Projection	Technical report	n: 9	Accuracy, correctly identified perforators	CTA and Doppler US
Ogunleye et al., 2022 [20]	Anatomical model	Retrospective study	n: 27	Flap harvest time, complications	CTA
DeFazio et al., 2020 [21]	Anatomical model	Retrospective study	n: 50, Study group: 9, Control group: 41	Accuracy, complications	CTA
Chae et al., 2021 [22]	Template	Prospective study	n: 20	Accuracy, operation time, usability, complications	CTA and Doppler US
Gómez-Cía et al., 2009 [23]	Template	Prospective study	n: 12	No. of selected perforators, accuracy	CTA

AR = Augmented Reality, HMD = Head Mounted Device, MRA = Magnetic Resonance Angiography, VST = Video-see-through, Doppler US = Doppler Ultrasound, RCT = Randomized Controlled Trial, CTA = Computed Tomographic Angiography, VR = Virtual Reality, 3D = 3-dimensional

3.3 Investigated techniques

Figure 2 illustrates the different techniques investigated in the articles. AR projects the patient's perforator anatomy as a 3D hologram, enabling its visualization in the real world. AR is categorized into three types: projection-based, video-see-through (VST), and optical-see-through (OST) [26]. OST AR also provides touchless interaction with the holograms, making it suitable for sterile environments [25]. For the 3D printed anatomical model, the patient's perforator anatomy is converted into a virtual 3D model and 3D printed, offering an enhanced understanding of vascular anatomy during surgery. Templates translate anatomical information onto the patient by placing the template on the patient's abdomen and outlining the perforator's course using holes or lines in the template. Templates can be produced using 3D printing or conventional printing methods on transparent paper.

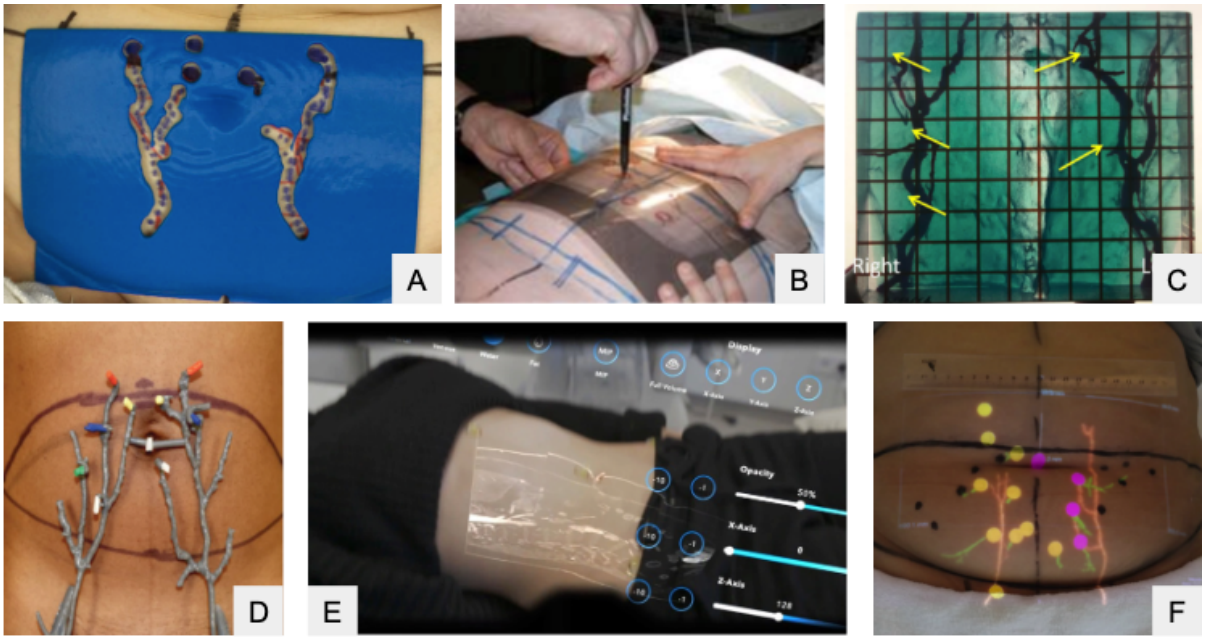

Figure 2 - Overview of the investigated techniques as illustrated in the articles. (A) 3D-printed template, (B) conventional printed template, (C, D) 3D printed anatomical model, (E) optical see-through Augmented Reality, (F) Projection-based Augmented Reality. For the video-see-through technique, no image was provided in the articles.

3.3.1 Augmented Reality

AR emerged as tool for mapping in four articles [16]-[19], offering an interactive, realistic, and intuitive understanding of anatomical structures. Berger et al. [16] explored OST AR, employing a Head-Mounted Device (HMD) to project MRI/MR-a images onto the patient. The article of Fitoussi et al. [17] used the video-see-through technique, visualizing the AR model on a digital tablet. The articles from Hummelink et al., [18], [19] developed a projection-based technology displaying the virtual perforator plan on the patient's skin. Three articles [17]-[19] designed a virtual 3D model based on CTA scans, the article from Berger et al. [16] employed MRA data. The holograms depicted the branching pattern of the DIEA and its significant perforators. In two articles [18], [19], the more substantial perforators (those with a diameter > 1mm) were marked with arrows. Particularly one article [19] annotated the most favorable perforators for the procedure. None of the articles extended their visualization to include other anatomical structures, such as the rectus abdominis and pyramidalis muscles and the skin.

3.3.2 3D printed anatomical model

Two articles described the implementation of 3D-printed anatomical models for perforator mapping [20], [21]. Anatomical models enhance the spatial visualization of anatomical structures, offering an advantage over the 2D visualization of data [27]. In both articles, the DIEA along with the trajectory and branching pattern of its perforators were reconstructed using CTA data. The article from DeFazio et al. [21] color-coded the perforators to correspond with their external diameters as seen on CTA. This approach aided in the identification of radiology dominant perforators, thereby assisting in guiding intraoperative decision-making.

3.3.3 Template

The utilization of a template was described in two articles [22], [23] and constitutes a straightforward method for post-processing CTA data into a tool for perforator mapping. Other than the anatomical models described before, the template only provides spatial information from one perspective (i.e., missing the in-depth relationship of perforators to each other and other structures). Chae et al. [22] employed CTA data to create a virtual 3D model of the patient's abdominal wall in the design of the template. Subsequently, holes and lines were created at the location of the DIEA and its significant perforators and the template was 3D printed. An overview of this process can be found in Figure 3. The article from Gómez-Cía et al. [23] printed the virtual reconstructed 3D model, including measurements of the distance from the umbilicus to the perforators, on a transparent template scale. This template allowed for preoperative transposition of the position of the perforators onto the patient's skin.

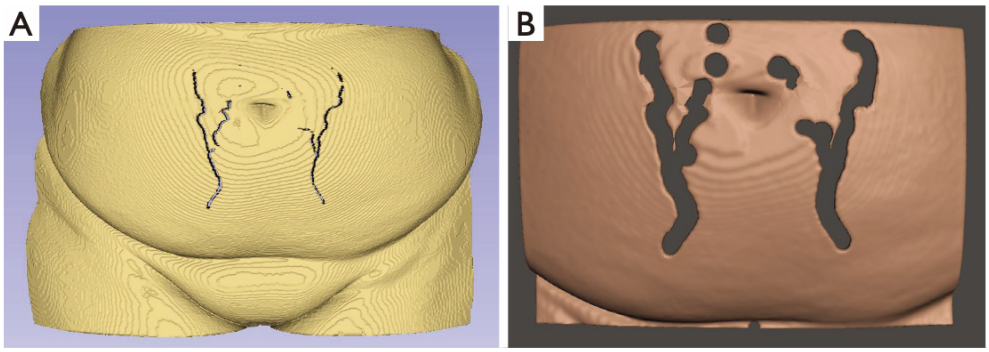

Figure 3 - (A) 3D image of the abdominal wall, holes and lines are placed appropriately to indicate the location of DIEA perforators, their intramuscular course and the DIEA pedicle. (B) Cropped 3D image into appropriate size with the holes/lines enlarged to fit marking pens.

3.4 Alignment

For AR, templates, and in one article [21] for the anatomical model, alignment of the preoperative planning with the patient's anatomy is essential for accurate information transfer to the patient's body. Two studies employed manual alignment [16], [19] in AR. The study by Berger et al. [16] aligned the hologram by overlaying anatomical landmarks and fiducials on the processed data to match the patient's actual body. These landmarks included the xiphoid process, umbilicus, and both anterior superior iliac spinae. Additionally, fiducials placed prior to scanning were visible on MRI/MR-A images, the 3D-surface scan, and the patient's body. In Hummelink et al.'s study [19], alignment was performed using the umbilicus and a predefined guideline as reference points. Two studies [17], [18] implemented automatic alignment, utilizing temporarily placed markers. Fitoussi et al. [17] used a single tracker, while Hummelink et al. [18] used four black-and-white markers positioned on specific anatomical

landmarks of the patient, including the umbilicus, symphysis, and bilateral anterior superior iliac spines.

DeFazio et al. [21] utilized their anatomical models as templates by orienting the models' reference limbs at the umbilical center point to outline the perforators on the patient. Conversely, Ogunleye et al. [20] did not report using their anatomical model as a template, therefore not describing any alignment process. To improve the alignment of the template with the patient, Chae et al. [22] marked a notch at the location of the pubic symphysis. This, along with the umbilicus, served as key anatomical reference points to ensure the accurate placement of the template on the patient's body.

3.5 Outcomes

In the reviewed articles, five different quantitative outcome measures were identified. A schematic overview of the outcomes per technique can be found in Appendix B.

3.5.1 Accuracy

Six articles [17]–[19], [21]-[23] evaluated the accuracy of the investigated technique by comparing it with Doppler US, CTA, or intra-operative findings. Four articles [19], [21]-[23] specifically evaluated the precision of estimated preoperative perforator markings by comparing them with the actual locations of perforators observed during surgery. The preoperative coordinates were collected for skin markings or perforator model locations, while intraoperative coordinates were collected from the perforators' points of emergence at the fascia. In both cases, the umbilicus was used as a reference point for the measurements. The discrepancy between preoperative and intraoperative perforator locations was referred to as the Margin of Error (MOE). An example of the preoperative perforator markings on the skin, the measurements on the anatomical model, and intraoperative measurements shown in the article from DeFazio et al. [21] is illustrated in Figure 4. A comprehensive overview of the accuracy evaluation outcomes can be found in Table 2.

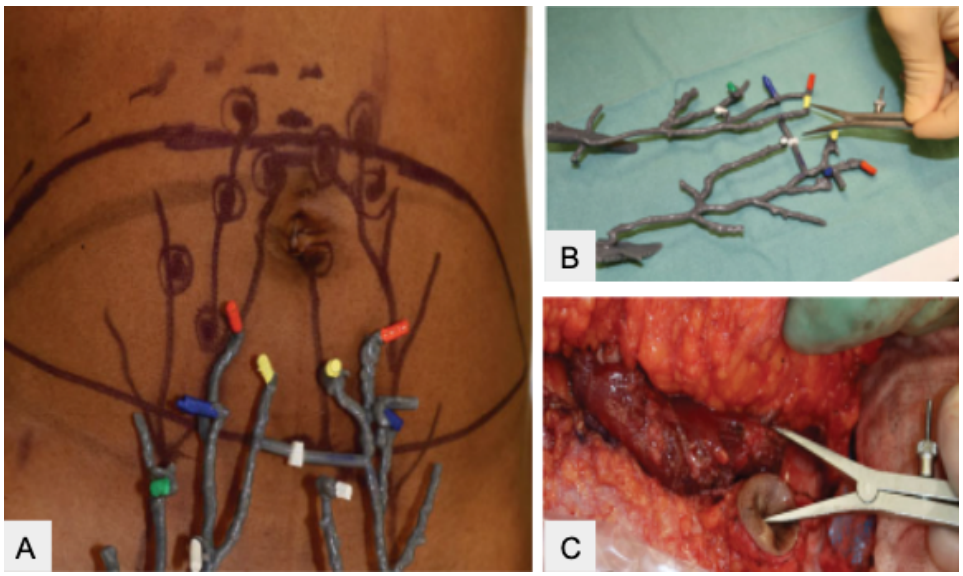

Figure 4 – (A) Perforator location markings on the patients skin based on the anatomical model. (B) Measurements of perforator location on the anatomical model, the distance between each perforator and the umbilical reference limb (i.e., center point of the umbilicus) was measured. (C) Measurement of the location of the clinically dominant perforator with the umbilicus as reference point.

Three studies [19], [21], [23] made a comparative analysis for the average distance from the planned to the actual intraoperative perforator location for the investigated technique and CTA or Doppler US. Hummelink et al [19] used the AR projection method for the preoperative perforator marking in the study group. In the control group, a handheld Doppler device was used to assess the perforator locations and all sounds representative of perforators were marked on the skin of the patients. CTA scans were available, but no virtual plans were created in this group. The article reported an average distance from the preoperative perforator markings on the skin to the actual intraoperative perforator locations of 7 ± 4 mm for Doppler US and 4 ± 3 mm for the projection method, demonstrating a statistically significant difference ($p = 0.009$) in favor of the projection method's accuracy. DeFazio et al. [21] reported a significantly lower distance in the perforator localization using markings from the anatomical model compared to markings that only used CTA data (0.81 mm versus 8.71 mm, $p < 0.0001$). Furthermore, the study presented that 90% of abdominal flaps mapped with the anatomical model were successfully harvested as true DIEP flaps, in contrast to only 58.6% when mapped using CTA alone ($p = 0.08$). This suggests the anatomical model's effectiveness in identifying dominant and optimally located perforators, thereby reducing the likelihood of intraoperative challenges that require switching to an alternative flap type. Gómez-Cía et al. [23] presented an average error rate of 2.3 mm (95% CI, 1.7–3.0) comparing coordinates from the perforators in the 3D abdominal wall reconstruction versus intra-operative measurements. In comparison, the authors referred to previous literature that indicated an average error margin of 5 mm for conventional CTA [28]. The study did not present a statistically significant p-value.

Three studies [16], [17], [22] made the comparative analysis of the average distance from the intraoperative perforator only for their investigated technique. Chae et al. [22] confirmed the template's accuracy by measuring the perforator's horizontal and vertical distance from the base of the umbilicus for the dominant perforators from the template. The article reported no statistical difference between the template-based locations and intraoperative findings (horizontal and vertical distances; $p = 0.09$ and 0.87, respectively). Additionally, the comparison between the template, handheld Doppler, and CTA measurements showed no significant statistical differences (horizontal and vertical distances; $p = 0.42$ and 0.74, respectively). Berger et al. [16], and Fitoussi et al. [17] utilized a different accuracy evaluation by measuring the distance between the preoperatively marked locations of the perforators for AR and Doppler US. For Berger et al. [16], a distance less than 40 mm between the markings based on AR and the perforator locations based on the MRA was defined as clinically acceptable. 23 out of 24 perforator distances were within the limits of the defined offset (96%). Fitoussi et al. [17] set this criterion at less than 10 mm. Their findings showed a median distance of 2 mm between the Doppler and AR landmarks, with 92% of AR landmarks falling within 10 mm of the Doppler landmarks.

Table 2 - Accuracy outcomes. Two different accuracy evaluation methods were described.

Author	Technique	Accuracy evaluation method	Outcome study group	Outcome control group	p-value
Hummelink et al., 2015 [19]	AR projection	Margin of Error*	4 ± 3 mm	7 ± 4 mm	p = 0.009 AR vs Doppler US
DeFazio et al., 2020 [21]	Anatomical model	Margin of Error	0.81 mm	8.71 mm	p < 0.0001 Anatomical model vs CTA
Gómez-Cía et al., 2009 [23]	Template	Margin of Error	2.3 mm (95% CI, 1.7–3.0 mm)	5 mm	NA Template vs virtual planning
Chae et al., 2021 [22]	Template	Margin of Error	NA	NA	p = 0.09 (horizontal) p = 0.87 (vertical) Template vs intraoperative
Berger et al., 2023 [16]	AR HMD	Distance between the marking on the skin to the perforator location on MRA <40mm	96%	NA	NA
Fitoussi et al., 2021 [17]	AR tablet	Distance between AR and Doppler marking on the skin <10mm	92%	NA	NA

AR = Augmented Reality, Doppler US = Doppler Ultrasound, 3D = 3-dimensional, CTA = Computed Tomographic Angiography, VR = Virtual Reality, NA = Not Available
**Margin of Error = the average distance from the preoperative markings on the skin at the estimated locations of the perforators, compared to the actual intraoperative locations of the perforators.*
The study group used the investigated technique in the preoperative mapping, the control group used CTA and Doppler US in the preoperative mapping.

3.5.2 Correctly identified perforators

Hummelink et al. [18], [19] focused on the accurate identification of perforators, examining the correlation between the number of perforators predicted preoperatively and the true number of perforators found intraoperatively. Hummelink et al. [19] showed that the number of correctly identified perforators was 56.9% ± 31.4% using the conventional Doppler US, versus 84.3% ± 25.8% (p = 0.030) for the projection group. For Hummelink et al. [18], Doppler US group achieved a 41.2% ± 8.2% accuracy rate while the projection group showed an accuracy rate of 61.7% ± 7.3% (p = 0.020). DeFazio et al. [21] showed complete agreement between the 3D-printed model and surgical observations regarding the number of perforators. Additionally, the anatomical model's preoperative identification of the DIEA's perforator origin and branching pattern was confirmed to match all observed intraoperative findings. By comparison, CTA interpretation of these parameters inaccurately identified the branching pattern and perforator origin in 3 cases (33%, p = 0.045 and p = 0.02, respectively). Inconsistencies between the interpretation of the preoperative CTA and the 3D-printed model resulted in changes to flap design and perforator selection in three patients (33%). A comprehensive overview of the perforator identification outcomes can be found in Table 3.

Table 3 – Comparative accuracy of correct preoperative perforator identification.

Author	Technique	Accuracy evaluation method	Outcome study group	Outcome control group	p-value
Hummelink et al., 2019 [18]	AR projection	Number of correctly identified perforators	61.7% ± 7.3%	41.2% ± 8.2%	p = 0.020
Hummelink et al., 2015 [19]	AR projection	Number of correctly identified perforators	84.3% ± 25.8%	56.9% ± 31.4%	p = 0.030
DeFazio et al., 2020 [21]	Anatomical 3D model	Number of correctly identified perforators	100%	67%	p = 0.045 and p = 0.02

AR = Augmented Reality.
The study group used an AR projection or anatomical model in the preoperative mapping, the control group used CTA and Doppler US in the preoperative mapping.

3.5.3 Time

Three studies [18], [20], [22] evaluated operative time as an outcome. A distinction was made between preoperative time, referring to the period needed for perforator identification and marking on the skin, and intra-operative time, covering the duration of flap harvest or dissection. A comprehensive overview of the time evaluation outcomes can be found in Table 4.

Looking into preoperative efficiency, Hummelink et al. [19] showed that the time taken for complete perforator identification and marking averaged 20.0 ± 5.5 minutes in the Doppler US group, in contrast to 2.3 ± 0.8 minutes for the projection method, marking a reduction of 17.7 minutes ($p < 0.001$). Chae et al. [22] reported a decrease in perforator identification and marking time from 22.36 minutes in the Doppler US and CTA group to 15.07 minutes in the template group, resulting in a significant reduction of 7.29 minutes ($p = 0.02$).

All three articles assessed the impact of the applied techniques on intra-operative efficiency. Hummelink et al. [18] noted a significant reduction in flap harvesting time from 155 ± 7 minutes in the Doppler US group to 136 ± 7 minutes in the projection group, resulting in a reduction of 19 minutes ($p = 0.012$). Chae et al. [22] found no statistically significant difference in the mean intramuscular dissection time, reporting 93.95 minutes for Doppler US and CTA versus 79.62 minutes for the template group ($p=0.34$). Similarly, Ogunleye et al. [20] reported no significant reduction in flap harvesting time, reporting 122.1 minutes for CTA versus 121.1 minutes for the anatomical model ($p = 0.844$).

Table 4 - Time evaluation methods and outcomes. Distinction between preoperative and intra-operative time measurements.

Author	Technique	Time evaluation method	Outcome study group	Outcome control group	p-value
Hummelink et al., 2019 [18]	AR projection	Preoperative perforator identification and marking time	2.3 ± 0.8 minutes	20.0 ± 5.5 minutes	p < 0.001
		Flap harvest time	136 ± 7 minutes	155 ± 7 minutes	p = 0.012
Chae et al., 2021 [22]	Template	Preoperative perforator identification and marking time	15.07 minutes	22.36 minutes	p = 0.02
		Intramuscular dissection time	79.62 minutes	93.95 minutes	p = 0.34
Ogunleye et al., 2022 [20]	Anatomical model	Flap harvest time	121.1 minutes	122.1 minutes	p = 0.844

AR = Augmented Reality
The study group used their investigated technique in the preoperative mapping, the control group used CTA and Doppler US in the preoperative mapping.

3.5.4 Complications

Four articles [18], [20]–[22] described the occurrence of flap loss as an outcome. For all four articles, there was no significant difference in flap loss between patients who underwent perforator mapping using the investigated technique versus CTA and/or Doppler US.

3.5.5 Usability

Two articles [16], [22] assessed the usability of the investigated technique. Studies used different metrics to evaluate the user experience with intraoperative use. Berger et al. [16] employed the system usability scale (SUS) and presented a total mean score of 67 ± 10 (max score = 100). This SUS score indicates 'moderate to good' usability, according to the interpretation scale [29]. Chae et al. [22] utilized a 5-part survey that assessed the perceived utility of the template on a 10-score scale. This score showed that the template was useful for preoperative marking (mean score: 8.6/10) and planning (7.9/10). However, it was not useful for intramuscular dissection (5.9/10) and, as a result, did not influence clinical management significantly (5.3/10). The surgeons appeared enthused about its potential and were keen to use the template again (8.8/10).

1. Discussion

This comparative review aimed to present a comprehensive analysis of post-processing techniques for intra-operative perforator mapping employed in DIEP flap reconstructive breast surgery. The included articles highlighted significant advancements in the field, particularly in the use of AR, 3D printed anatomical models, and templates, and presented quantitative outcomes for practical efficiency and utilization.

4.1 Interpretation of results

Among the techniques reviewed, AR showed the most promising results, demonstrating superior accuracy and time efficiency. AR outperformed the conventional Doppler US method in preoperatively identifying perforators, showing a higher agreement with the actual number of perforators found during surgery. The AR projection method also showed a smaller average distance from the preoperative planned markings to the actual intraoperative perforator locations compared to Doppler US, coupled with a significant reduction in both preoperative and intraoperative time by approximately 20 minutes. This suggests that AR not only enhances the surgeon's ability to accurately map and identify critical perforators but also increases surgical efficiency.

The utilization of 3D-printed anatomical models showed a significantly lower distance between the preoperative planned markings on the patient's skin and the actual intraoperative perforator locations compared to the preoperative marking using only CTA. However, the implementation of these models did not demonstrate a statistically significant reduction in intraoperative time. The transition from 2D to 3D visualization has been confirmed to enhance the visualization of anatomical structures, increasing the surgeon's proficiency in tracking vascular pathways, assessing their proximity to anatomical landmarks and evaluating their course [27], [31].

Templates showed correct perforator marking, leading to quicker preoperative identification of perforators. Despite this efficiency, the utilization of a template did not provide additional

anatomical insights beyond what is offered by CTA and Doppler US. Their accuracy was comparable to these traditional methods, indicating that while templates improve the efficiency of the preoperative process, they did not necessarily offer superior precision.

Among the studies reviewed, three articles considered the usability of the investigated technique as a quantitative outcome measure. Notably, the study by Berger et al. [16] stands out as the only research that utilized a standardized and validated questionnaire to assess usability. While the accuracy and time reduction offered by these techniques are crucial factors for their adoption in clinical practice, the importance of usability as a parameter for technology assessment should not be underestimated. Usability encompasses key aspects such as effectiveness, efficiency, memorability, and applicability, all of which are essential for the successful integration of new technologies into surgical workflows [32].

4.2 Previous literature

The previous review from Steenbeek et al., [12] provided a broad overview of alternative perforator mapping modalities in free-flap breast reconstructive surgery. This new review delved deeper, offering new insights into the evaluation of these techniques by presenting the quantitative outcomes described in the reviewed articles.

This review showed a notable inconsistency in how different studies measure outcomes, revealing a lack of standardization in evaluating the effectiveness of the techniques discussed. The methods used to define and measure efficacy vary significantly from one study to another. For example, while some articles focused on measuring the distance from the preoperatively planned to the actual intraoperative perforator locations, others assessed the proportion of correctly identified perforators. Additionally, this review highlighted the innovative use of AR in breast reconstruction surgery. While previous literature acknowledged the potential of this technology, this review provided concrete evidence of its benefits, particularly in enhancing accuracy and improving time efficiency.

4.2 Strengths and limitations

The strength of this review lies in its comprehensive approach, encompassing a wide range of innovative techniques and providing a complete overview of current technological advancements in the field. Thereby, an overview is giving of the outcomes of the articles, making it possible to compare different techniques. However, the review faces limitations due to the variability in study designs, population sizes, and outcome measures across the included studies, which may affect the generalizability of the results. Furthermore, no comprehensive quality assessment was performed for the included studies and their methodologies.

4.3 Recommendations

This review highlights a gap in quantitative research on post-processing techniques in DIEP flap reconstructive breast surgery, despite a recent growth in publications. While the application of AR demonstrated promising results for perforator mapping in DIEP flaps, quantifiable results have only been documented for the projection method. Particularly, the use of Augmented Reality Head-Mounted Devices (AR HMD) showed promising results in plastic surgery and other surgical disciplines [33], yet its application in soft tissue interventions remains underexplored.

The utilization of the HoloLens 2 (Microsoft, Redmond, WA, USA) for creating holograms in perforator mapping for DIEP flap surgery, as described by studies from Pratt et al. [34] and Wesselius et al., [35] demonstrated superior outcomes compared to traditional Doppler US. These studies underscored the potential of AR HMD in enhancing intraoperative visualization of anatomical structures, such as vessels, directly on the patient. However, neither of these articles reported the practicability, usability, and accuracy of these holograms in breast surgery. Moreover, while Berger et al. [16] showed results regarding usability, their study did not encompass the creation of a virtual 3D model and employed Magnetic Resonance Angiography (MRA) data instead of the more commonly used Computed Tomography Angiography (CTA) data.

Future research should focus on the practical application and usability of AR HMD technologies, like the HoloLens, in DIEP flap breast reconstruction surgery. This research should not only evaluate the technical efficacy but also delve into the integration into surgical workflows, ease of use, and overall impact on the surgical process. This includes assessing the learning curve for surgeons, and its effectiveness in improving surgical outcomes compared to traditional methods. Examples of potential outcome measures could be preoperative mapping times, the concordance between the preoperative choice of best perforator and the intraoperative used perforator, margins of error for planned and intraoperative perforators, and validated usability scores.

4. Conclusion

In conclusion, techniques that employ post-processing volumetric datasets (from CTA or MRA) for perforator mapping in DIEP flap breast reconstruction surgery is an emerging area of research. Although various techniques are described in literature, few articles present quantitative results regarding the application and effectiveness of the investigated techniques. New techniques aspire to make 3D data practical for direct visualization in pre- and intraoperative settings, resulting in a better understanding of the vascular anatomy during surgery. As AR emerges as a particularly promising method in perforator mapping, future research should focus on the practical implementation and effectiveness of AR HMD technologies in DIEP flap breast reconstruction surgery. A clinical study evaluating the usability and added value of AR in the visualization and translation of the preoperative planning to the patient's anatomy would be of high value.

5. References

[1] Smolarz B, Nowak AZ, Romanowicz H. Breast cancer—epidemiology, classification, pathogenesis and treatment (review of literature). Cancers. 2022;14(10):2569.
[2] Sung H, Ferlay J, Siegel RL, Laversanne M, Soerjomataram I, Jemal A, et al. Global cancer statistics 2020: GLOBOCAN estimates of incidence and mortality worldwide for 36 cancers in 185 countries. CA: a cancer journal for clinicians. 2021;71(3):209-49.
[3] Boughey JC, Attai DJ, Chen SL, Cody HS, Dietz JR, Feldman SM, et al. Contralateral prophylactic mastectomy (CPM) consensus statement from the American Society of Breast Surgeons: data on CPM outcomes and risks. Annals of surgical oncology. 2016;23:3100-5.
[4] Ng SK, Hare RM, Kuang RJ, Smith KM, Brown BJ, Hunter-Smith DJ. Breast reconstruction post mastectomy: patient satisfaction and decision making. Annals of plastic surgery. 2016;76(6):640-4.
[5] Howard-McNatt MM. Patients opting for breast reconstruction following mastectomy: an analysis of uptake rates and benefit. Breast Cancer: Targets and Therapy. 2013:9-15.
[6] Toyserkani NM, Jørgensen MG, Tabatabaeifar S, Damsgaard T, Sørensen JA. Autologous versus implant-based breast reconstruction: A systematic review and meta-analysis of Breast-Q patient-reported outcomes. Journal of Plastic, Reconstructive & Aesthetic Surgery. 2020;73(2):278-85.
[7] Saldanha IJ, Broyles JM, Adam GP, Cao W, Bhuma MR, Mehta S, et al. Autologous breast reconstruction after mastectomy for breastcancer: a systematic review. Plastic and Reconstructive Surgery Global Open. 2022;10(3).
[8] Garvey PB, Buchel EW, Pockaj BA, Casey III WJ, Gray RJ, Hern´andez JL, et al. DIEP and pedicled TRAM flaps: a comparison of outcomes. Plastic and reconstructive surgery. 2006;117(6):1711-9.
[9] Kiely J, Kumar M, Wade RG. The accuracy of different modalities of perforator mapping for unilateral DIEP flap breast reconstruction: a systematic review and meta-analysis. Journal of Plastic, Reconstructive & Aesthetic Surgery. 2021;74(5):945-56.
[10] Miranda BH, Pywell M, Floyd D. A preoperative marking template for deep inferior epigastric artery perforator flap perforators in breast reconstruction. Archives of Plastic Surgery. 2014;41(02):171-3.
[11] Galstyan A, Bunker MJ, Lobo F, Sims R, Inziello J, Stubbs J, et al. Applications of 3D printing in breast cancer management. 3D printing in medicine. 2021;7(1):1-10.
[12] Steenbeek LM, Peperkamp K, Ulrich DJ, Hummelink S. Alternative imaging technologies for perforator mapping in free flap breast reconstructive surgery–A comprehensive overview of the current literature. Journal of Plastic, Reconstructive & Aesthetic Surgery. 2022;75(11):4074-84.
[13] Ireton JE, Lakhiani C, Saint-Cyr M. Vascular anatomy of the deep inferior epigastric artery perforator flap: a systematic review. Plastic and reconstructive surgery. 2014;134(5):810e-821e.
[14] Lam D, Mitsumori L, Neligan P, Warren B, Shuman W, Dubinsky T. Pre-operative CT angiography and three-dimensional image post processing for deep inferior epigastric perforator flap breast reconstructive surgery. The British Journal of Radiology. 2012;85(1020):e1293-7.
[15] Jiang T, Yu D, Wang Y, Zan T, Wang S, Li Q. HoloLens-based vascular localization system: precision evaluation study with a three-dimensional printed model. Journal of medical Internet research. 2020;22(4):e16852.
[16] Berger MF, Winter R, Tuca AC, Michelitsch B, Schenkenfelder B, Hartmann R, et al.

Workflow assessment of an augmented reality application for planning of perforator flaps in plastic reconstructive surgery: Game or game changer? Digital Health. 2023;9:20552076231173554.
[17] Fitoussi A, Tacher V, Pigneur F, Heranney J, Sawan D, Dao TH, et al. Augmented reality-assisted deep inferior epigastric artery perforator flap harvesting. Journal of Plastic, Reconstructive & Aesthetic Surgery. 2021;74(8):1931-71.
[18] Hummelink S, Hoogeveen YL, Kool LJS, Ulrich DJ. A new and innovative method of preoperatively planning and projecting vascular anatomy in DIEP flap breast reconstruction: a randomized controlled
trial. Plastic and reconstructive surgery. 2019;143(6):1151e-1158e.
[19] Hummelink S, Hameeteman M, Hoogeveen Y, Slump C, Ulrich D, Kool LS. Preliminary results using a newly developed projection method to visualize vascular anatomy prior to DIEP flap breast reconstruction. Journal of plastic, reconstructive & aesthetic surgery. 2015;68(3):390-4.
[20] Ogunleye AA, Deptula PL, Inchauste SM, Zelones JT, Walters S, Gifford K, et al. The utility of three dimensional models in complex microsurgical reconstruction. Archives of plastic surgery. 2020;47(05):428-34.
[21] DeFazio MV, Arribas EM, Ahmad FI, Le-Petross HT, Liu J, Chu CK, et al. Application of Three-Dimensional Printed Vascular Modeling as a Perioperative Guide to Perforator Mapping and Pedicle Dissection during Abdominal Flap Harvest for Breast Reconstruction. Journal of Reconstructive Microsurgery. 2020;36(05):325-38.
[22] Chae MP, Hunter-Smith DJ, Chung RD, Smith JA, Rozen WM. 3D-printed, patient-specific DIEP flap templates for preoperative planning in breast reconstruction: a prospective case series. Gland Surgery. 2021;10(7):2192.
[23] G´omez-C´ıa T, Gacto-S´anchez P, Sicilia D, Su´arez C, Acha B, Serrano C, et al. The virtual reality tool VirSSPA in planning DIEP microsurgical breast reconstruction. International journal of computer assisted radiology and surgery. 2009;4:375-82.
[24] Zinser MJ, Kr¨oger N, Malter W, Schulz T, Puesken M, Mallmann P, et al. Preoperative Perforator Mapping in DIEP Flaps for Breast Reconstruction. The Impact of New Contrast-Enhanced Ultrasound Techniques. Journal of Personalized Medicine. 2022;13(1):64.
[25] Zhao Z, Poyhonen J, Chen Cai X, Sophie Woodley Hooper F, Ma Y, Hu Y, et al. Augmented reality technology in image-guided therapy: State-of-the-art review. Proceedings of the Institution of Mechanical Engineers, Part H: Journal of Engineering in Medicine. 2021;235(12):1386-98.
[26] Furman AA, Hsu WK. Augmented reality (AR) in orthopedics: current applications and future directions. Current reviews in musculoskeletal medicine. 2021:1-9.
[27] Jablonka EM, Wu RT, Mittermiller PA, Gifford K, Momeni A. 3-DIEPrinting: 3D-printed models to assist the intramuscular dissectionin abdominally based microsurgical breast reconstruction. Plastic and Reconstructive Surgery Global Open. 2019;7(4).
[28] Rozen W, Ashton M, Stella D, Phillips T, Taylor G. Stereotactic image-guided navigation in the preoperative imaging of perforators for DIEP flap breast reconstruction. Microsurgery: Official Journal of the International Microsurgical Society and the European Federation of Societies for Microsurgery. 2008;28(6):417-23.
[29] Bangor A, Kortum P, Miller J. Determining what individual SUS scores mean: Adding an adjective rating scale. Journal of usability studies. 2009;4(3):114-23.
[30] Jacobson NM, Carerra E, Treat A, McDonnell M, Mathes D, Kaoutzanis C. Hybrid modeling techniques for 3D printed deep inferior epigastric perforator flap models. 3D Printing in Medicine. 2023;9(1):26.

[31] Egozi D, Perkhulov V, Kouniavsky L, Loschope ADV, Benkler M, Benharush D. DIEP Flap Preoperative Planning Using Virtual Reality Based on CT Angiography. Plastic and Reconstructive Surgery Global Open. 2022;10(3).
[32] Assila A, Ezzedine H, et al. Standardized usability questionnaires: Features and quality focus. Electronic Journal of Computer Science and Information Technology. 2016;6(1).
[33] Sayadi LR, Naides A, Eng M, Fijany A, Chopan M, Sayadi JJ, et al. The new frontier: a review of augmented reality and virtual reality in plastic surgery. Aesthetic surgery journal. 2019;39(9):1007-16.
[34] Pratt P, Ives M, Lawton G, Simmons J, Radev N, Spyropoulou L, et al. Through the HoloLens™ looking glass: augmented reality for extremity reconstruction surgery using 3D vascular models with perforating vessels. European radiology experimental. 2018;2:1-7.
[35] Wesselius TS, Meulstee JW, Luijten G, Xi T, Maal TJ, Ulrich DJ. Holographic augmented reality for DIEP flap harvest. Plastic and reconstructive surgery. 2021;147(1):25e-29e

Appendix B – Study 1 Questionnaire

Conventionele CTA scan						
1	Wat is het aantal perforatoren dat u heeft geïdentificeerd?					
2	Ik kon de volgende perforator karakteristieken adequaat beoordelen:	Sterk mee oneens				Sterk mee eens
A.	**Kaliber**					
		1	2	3	4	5
B.	**Intramusculair verloop**					
		1	2	3	4	5
C.	**Perforator locaties in de lap**					
		1	2	3	4	5
D.	**Oorsprong van perforatoren**					
		1	2	3	4	5
E.	**Subcutaan vertakkingspatroon**					
		1	2	3	4	5
F.	**Locaties ten opzichte van elkaar**					
		1	2	3	4	5

3 Welke karakteristiek(en) was/waren het belangrijkst bij het selecteren van de perforator? (Meerdere antwoorden mogelijk)

A. Kaliber	**B. Intramusculair verloop**	**C. Locatie in lap**	**D. Oorsprong**	**E. Subcutaan vertakkingpatroon**	**F. Locatie t.o.v. andere perforatoren**

		Sterk mee oneens				Sterk mee eens
4	Ik kan met zekerheid zeggen dat ik de geselecteerde perforator daadwerkelijk ga gebruiken tijdens de operatie.					

3D model

1 Wat is het aantal perforatoren dat u heeft geïdentificeerd? ☐

2 Ik kon de volgende perforator karakteristieken adequaat beoordelen:

	Sterk mee oneens				Sterk mee eens
A. Kaliber	☐	☐	☐	☐	☐
	1	2	3	4	5
B. Intramusculair verloop	☐	☐	☐	☐	☐
	1	2	3	4	5
C. Perforator locaties in de lap	☐	☐	☐	☐	☐
	1	2	3	4	5
D. Oorsprong van perforatoren	☐	☐	☐	☐	☐
	1	2	3	4	5
E. Subcutaan vertakkingspatroon	☐	☐	☐	☐	☐
	1	2	3	4	5
F. Locaties ten opzichte van elkaar	☐	☐	☐	☐	☐
	1	2	3	4	5

3 Welke karakteristiek(en) was/waren het belangrijkst bij het selecteren van de perforator? (Meerdere antwoorden mogelijk)

A. Kaliber	**B. Intramusculair verloop**	**C. Locatie in lap**	**D. Oorsprong**	**E. Subcutaan vertakkingpatroon**	**F. Locatie t.o.v. andere perforatoren**
☐	☐	☐	☐	☐	☐

	Sterk mee oneens				Sterk mee eens
4 Ik kan met zekerheid zeggen dat ik de geselecteerde perforator daadwerkelijk ga gebruiken tijdens de operatie.	☐	☐	☐	☐	☐
	1	2	3	4	5

	Nee	Ja
5 Het 3D model is van toegevoegde waarde voor de preoperatieve planning van de DIEP lap ten opzichte van de CTA scan	☐	☐

6 Ik zou in de toekomst gebruik willen maken van:

☐ **A. Een 3D model in plaats van de conventionele scan**
☐ **B. Een 3D model als aanvulling op de conventionele scan**
☐ **C. Alleen de conventionele scan (geen 3D model)**

Augmented Reality

1 Wat is het aantal perforatoren dat u heeft geïdentificeerd? ☐

2 Ik kon de volgende perforator karakteristieken adequaat beoordelen:

	Sterk mee oneens				Sterk mee eens
A. Kaliber	☐ 1	☐ 2	☐ 3	☐ 4	☐ 5
B. Intramusculair verloop	☐ 1	☐ 2	☐ 3	☐ 4	☐ 5
C. Perforator locaties in de lap	☐ 1	☐ 2	☐ 3	☐ 4	☐ 5
D. Oorsprong van perforatoren	☐ 1	☐ 2	☐ 3	☐ 4	☐ 5
E. Subcutaan vertakkingspatroon	☐ 1	☐ 2	☐ 3	☐ 4	☐ 5
F. Locaties ten opzichte van elkaar	☐ 1	☐ 2	☐ 3	☐ 4	☐ 5

3 Welke karakteristiek(en) was/waren het belangrijkst bij het selecteren van de perforator? (Meerdere antwoorden mogelijk)

A. Kaliber	**B. Intramusculair verloop**	**C. Locatie in lap**	**D. Oorsprong**	**E. Subcutaan vertakkingpatroon**	**F. Locatie t.o.v. andere perforatoren**
☐	☐	☐	☐	☐	☐

	Sterk mee oneens				Sterk mee eens
4 Ik kan met zekerheid zeggen dat ik de geselecteerde perforator daadwerkelijk ga gebruiken tijdens de operatie.	☐ 1	☐ 2	☐ 3	☐ 4	☐ 5

	Nee	Ja
5 Augmented Reality is van toegevoegde waarde voor de preoperatieve planning van de DIEP lap ten opzichte van de CTA scan en het 3D model	☐	☐

6 Ik zou in de toekomst gebruik willen maken van:

☐ **A. Augmented Reality in plaats van de conventionele scan**

☐ **B. Augmented Reality als aanvulling op de conventionele scan**

☐ **C. Alleen de conventionele scan (geen Augmented Reality)**

Appendix C – Comments and additional remarks Study 1

Categories:
Recommendations 3D model
Confidence perforator choice
Advantages CTA scan
The added value of 3D visualization/AR

Recommendations 3D model

- When assessing the CTA scan, I look for dark areas in the muscle, which indicates fat tissue. When the perforator crosses the fat, I know this is easier to dissect. This is something that is currently missing in the 3D model.
- The umbilicus marker is located on the outside of the umbilicus, at the skin level. Especially in very obese patients, this can lead to inaccuracies in locating the true position of the umbilicus due to skin movement. A possible solution would be to create a 3D marker model at the point where the umbilicus connects with the fascia.

Confidence perforator choice:

- The 3D model or AR provides more information compared to the initial CTA scan. You make a better-informed decision, but this extra information can lead also to less confidence in selecting the perforator because you have more information to take into consideration.
- For a double-sided reconstruction (as opposed to a single), a perforator is needed on both sides. This increases confidence in the choice of perforator due to fewer options, but it does not necessarily make the overall decision easier.

Advantages of CTA scan:

- CTA scan offers a better view of the connecting venous pattern in the subcutaneous tissue. This is something that is also taken into consideration when planning the flap.
- When the CTA scan shows one very dominant perforator, the confidence in perforator choice is high. In these cases, the 3D model does not influence the perforator choice but offers extra information regarding the origin and intramuscular course.
- For abnormal anatomies besides the RA muscle or perforator anatomy, CTA images are necessary to take this information into account.

Advantages of 3D visualization/AR:

- The 3D visualization offers a better overview of the various connections between perforators, the perforator origin, and the intramuscular course.
- The 3D model gives a clear initial view of the anatomy, decreasing the time it takes to understand the anatomy. You can immediately see if it is one or multiple systems, and whether it is medially or laterally dominant.
- Using AR gives a better feeling and understanding of the 3D model because you can zoom in by bringing the 3D hologram closer to your eyes. This simulates the clinical situation, where the surgeon uses surgical loupes and is highly focused on the patient's perforator anatomy.
- When the RA muscle is switched to transparent in the 3D hologram, this offers a good view of the perforators and their intramuscular course. Because of the holographic projection, you can more clearly see the course of the perforator

Appendix D – 3D models and perforator labels (phase 1&2)

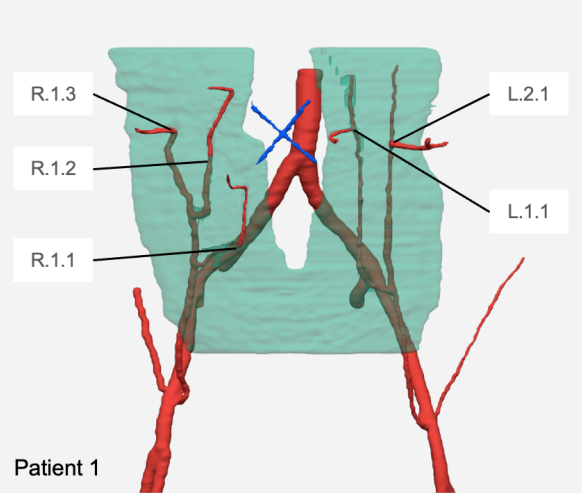

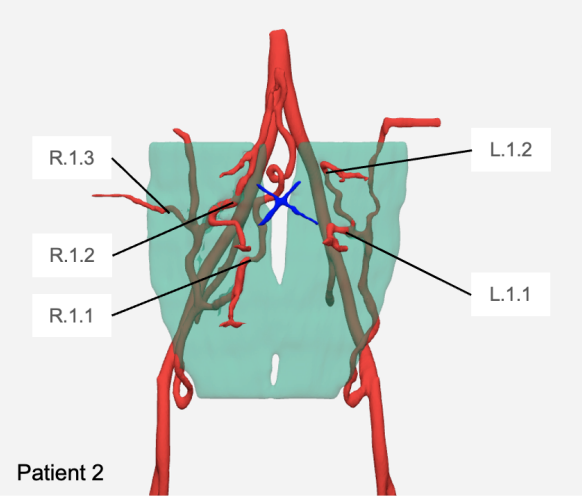

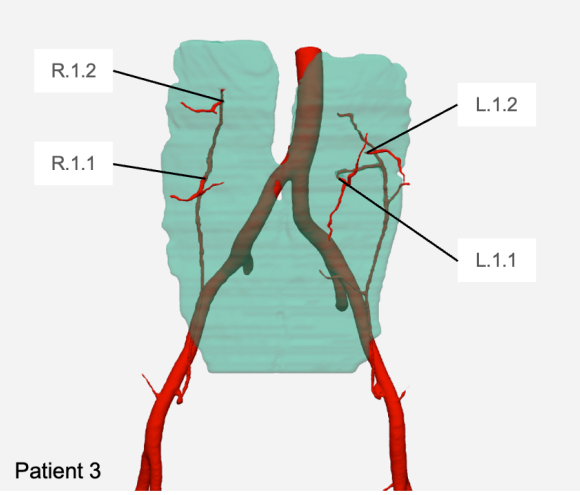

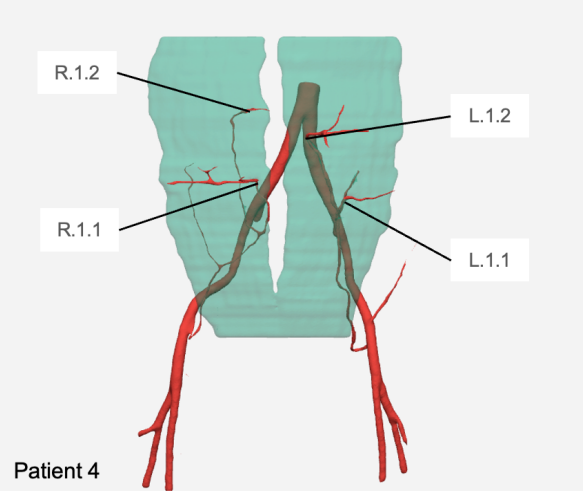

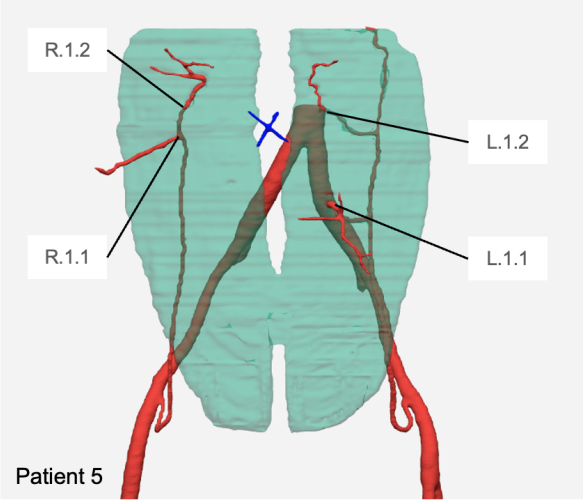

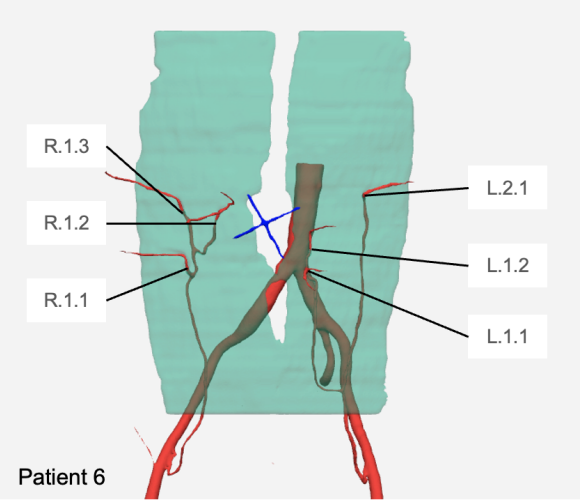

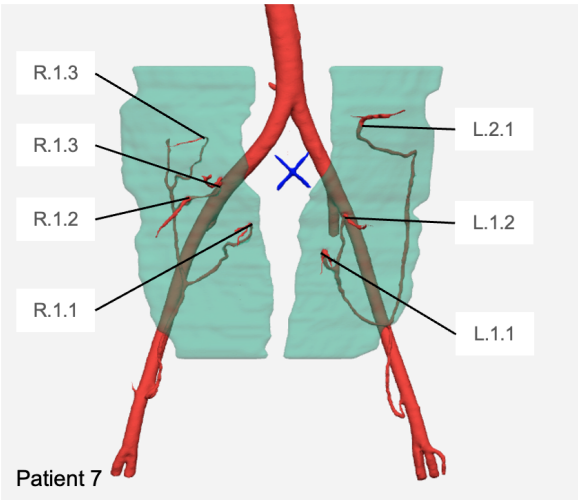
R.1.3
R.1.3
R.1.2
R.1.1
L.2.1
L.1.2
L.1.1
Patient 7

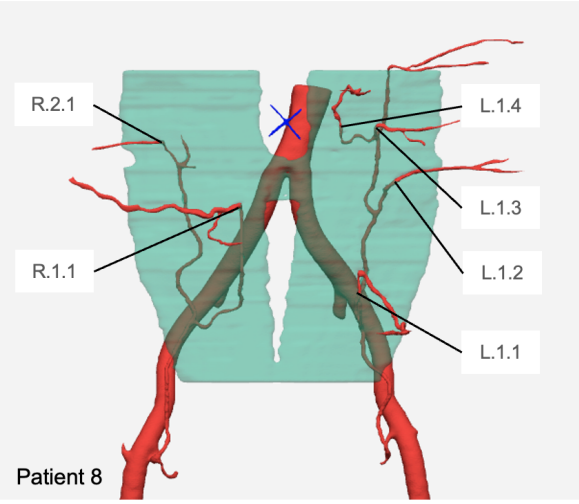
R.2.1
R.1.1
L.1.4
L.1.3
L.1.2
L.1.1
Patient 8

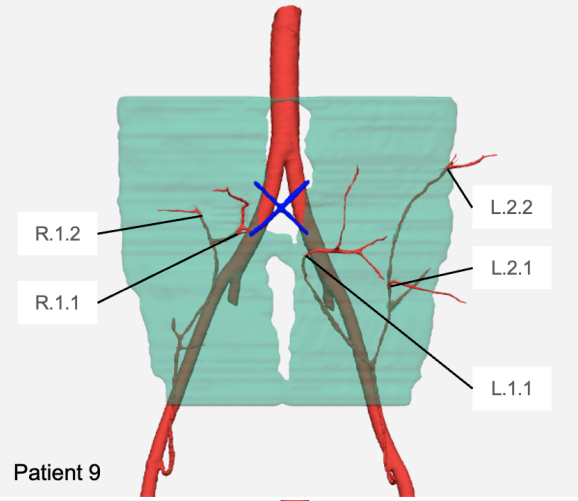
R.1.2
R.1.1
L.2.2
L.2.1
L.1.1
Patient 9

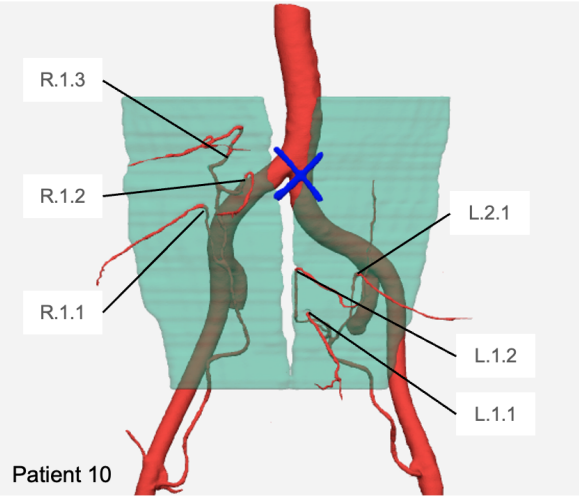
R.1.3
R.1.2
R.1.1
L.2.1
L.1.2
L.1.1
Patient 10

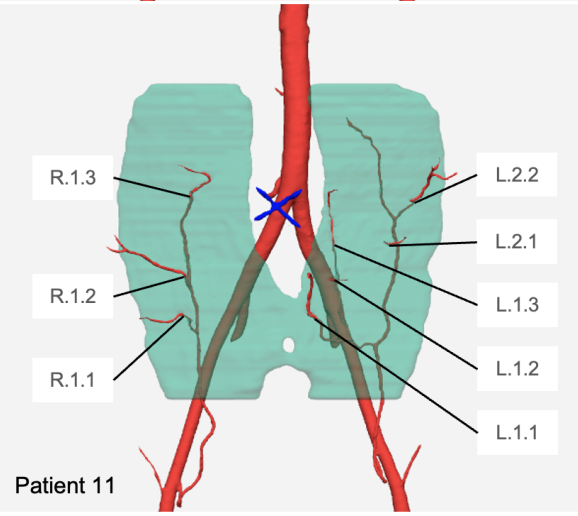
R.1.3
R.1.2
R.1.1
L.2.2
L.2.1
L.1.3
L.1.2
L.1.1
Patient 11

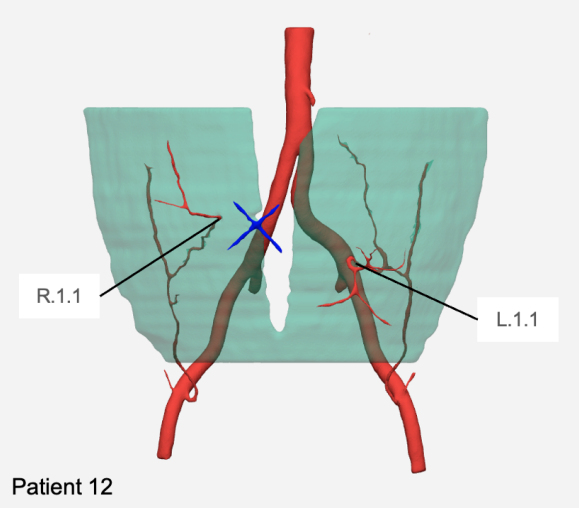
R.1.1
L.1.1
Patient 12

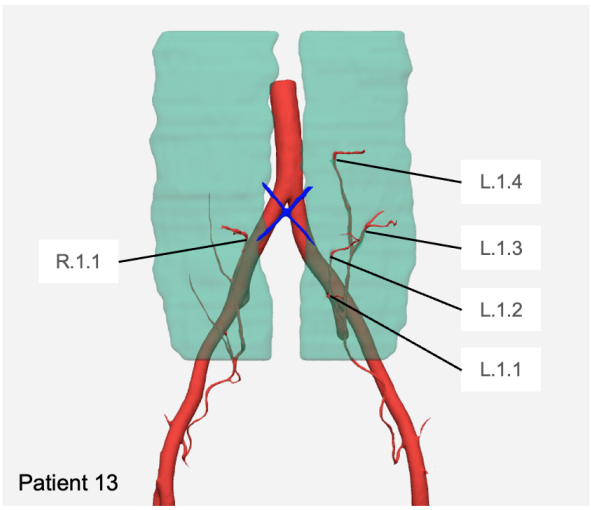
R.1.1
L.1.4
L.1.3
L.1.2
L.1.1
Patient 13

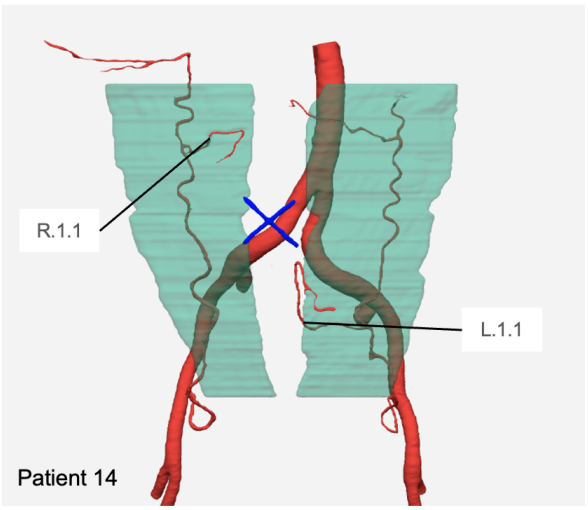
R.1.1
L.1.1
Patient 14

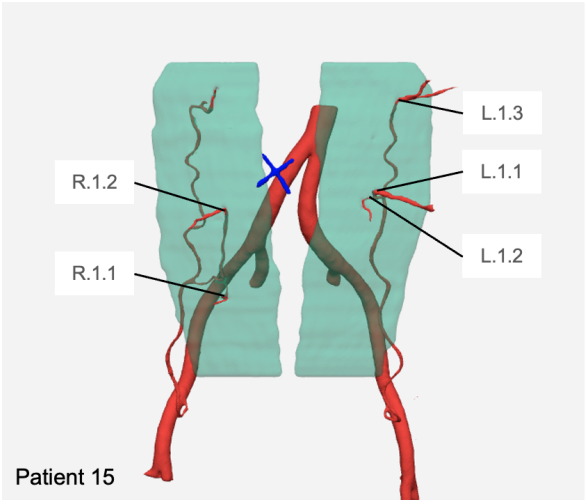
R.1.2
R.1.1
L.1.3
L.1.1
L.1.2
Patient 15

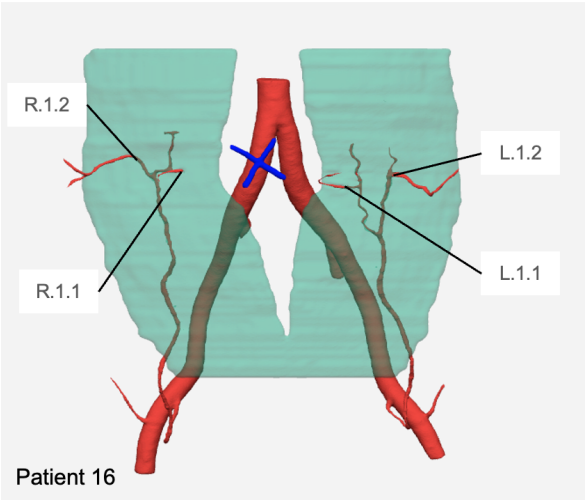
R.1.2
R.1.1
L.1.2
L.1.1
Patient 16

Appendix E – Study 2 Questionnaire

Postoperatief

1 De volgende perforator karakteristieken kwamen intra-operatief adequaat overeen met het AR model:

		Sterk mee oneens				Sterk mee eens
A.	**Kaliber**					
		1	2	3	4	5
B.	**Intramusculair verloop**					
		1	2	3	4	5
C.	**Perforator locaties in de lap**					
		1	2	3	4	5
D.	**Oorsprong van perforatoren**					
		1	2	3	4	5
F.	**Locaties ten opzichte van elkaar**					
		1	2	3	4	5

		Sterk mee oneens			Sterk mee eens	
5	Ik zou het Augmented Reality model in preoperatieve setting willen gebruiken.					
		1	2	3	4	5

System Usability Score (SUS-score)

		Sterk mee oneens				Sterk mee eens
1.	**Ik wil dit systeem vaker gebruiken**					
		1	2	3	4	5
2.	**Ik vond het systeem onnodig complex**					
		1	2	3	4	5
3.	**Ik vond het systeem makkelijk te gebruiken**					
		1	2	3	4	5
4.	**Ik heb technische ondersteuning nodig om dit systeem te gebruiken**					
		1	2	3	4	5
5.	**Ik vond de verschillende functies goed geïntegreerd in het systeem**					
		1	2	3	4	5
6.	**Er was te veel inconsistentie in het systeem**					
		1	2	3	4	5
7.	**Men kan het gebruik van dit systeem snel aanleren**					
		1	2	3	4	5
8.	**Ik vond het systeem erg omslachtig om te gebruiken**					
		1	2	3	4	5
9.	**Ik had veel zelfvertrouwen bij het gebruik van dit systeem**					
		1	2	3	4	5
10.	**Ik moest veel dingen leren voor ik aan de slag kon met dit systeem**					
		1	2	3	4	5

Appendix F – Segmentation & HoloLens guideline

Slicer
Segmentation in 3DSlicer

1. Import DICOM data into 3DSlicer

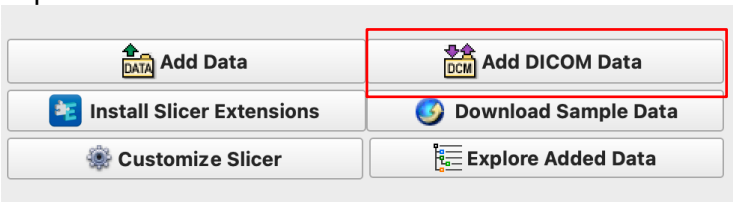

2. Go to **Segment Editor** module

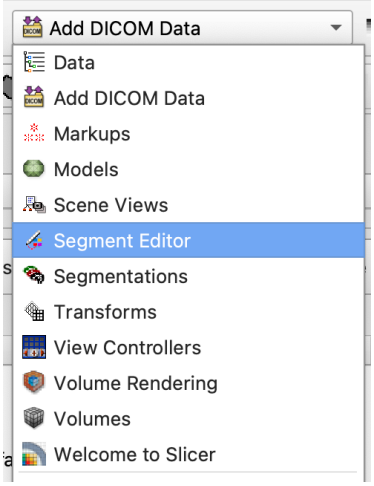

3. Select the 0.5cm CTA as Master Volume and click **Add** to create a new segmentation

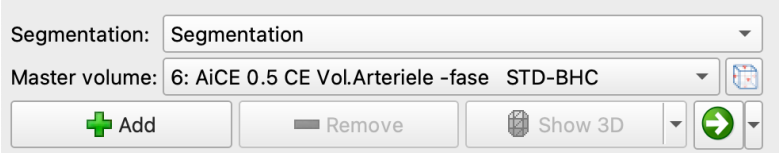

4. Segment the following structures:
    a) Fat
        1. Use **threshold**
        2. Update manually
        3. Smooth using Median/Opening/Closing
    b) Muscles (fill between slices)
        1. Use **fill between slices**
        2. Update manually
        3. Smooth using **Median/Opening/Closing**
    c) Perforators
        1. Use **threshold**
        2. Update manually
5. Go to the **Segmentation** module
    a) Export to files
    b) Change destination folder
    c. Export as STL

Mimics viewer

1. Click on **Add case**
2. Add the .mcs file
3. Open the Case

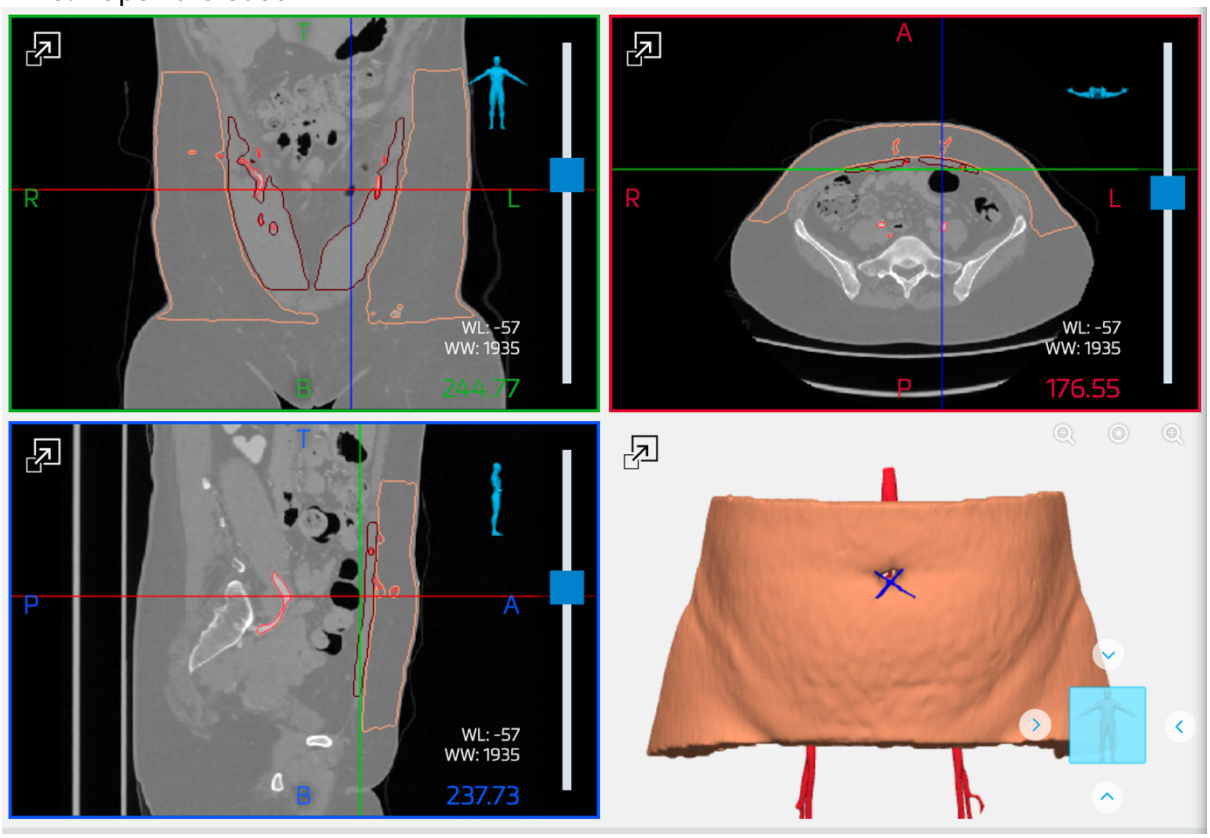

How to use Mimics viewer:

- Right mouse: turn 3D model around
- Scroll: zoom in and out
- Click the scrolling wheel: hold model and move around
- Use box in the right corner to get the basic viewing planes
- Click on the eye to view a segment or make it invisible
- Click on the box to make a segment transparent

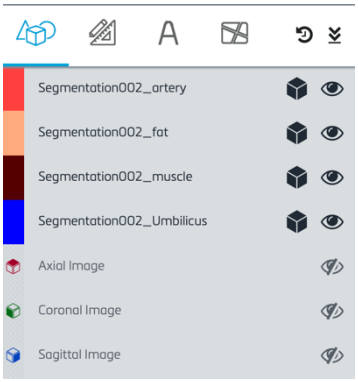

Study protocol

CT-scan on 2D screen

1. Open CTA scan in Hix
2. Search for correct patient
3. Examine CTA scan
4. Choose the optimal perforator
    a. *Observer: mark this in 3DSlicer*
    b. *Give name: CT_pt1_pp1 (CT, patient 1, person 1)*
5. Fill in questionnaire

3D-model on 2D screen

1. Open Mimics Viewer
2. Choose the correct patient
3. Examine 3D model in Mimics Viewer
4. Choose the optimal perforator
    a. *Observer: mark this in 3DSlicer*
    b. *Give name: 3D_pt1_pp1*
5. Fill in questionnaire

Augmented Reality

1. Start-up HoloLens
2. Open app: Mimics Viewer
3. Choose correct patient
4. Choose the optimal perforator
    a. *Observer: mark this in 3DSlicer*
    b. *Give name: HL_pt1_pp1*
5. Fill in questionnaire